Plant Physiology®

Association of the benzoxazinoid pathway with boron homeostasis in maize

Liuyang Chu,[1,†] Vivek Shrestha,[2,†] Cay Christin Schäfer,[1] Jan Niedens,[3] George W. Meyer,[2] Zoe Darnell,[2] Tyler Kling,[2]

Tobias Dürr-Mayer,[4] Aleksej Abramov,[5] Monika Frey,[5] Henning Jessen,[4] Gabriel Schaaf,[6] Frank Hochholdinger,[1]

Agnieszka Nowak-Król,[3] Paula McSteen,[2] Ruthie Angelovici,[2] Michaela S. Matthes[1,*]

[1]Institute of Crop Science and Resource Conservation, Crop Functional Genomics, University of Bonn, Friedrich-Ebert-Allee 144, Bonn 53113, Germany
[2]Division of Biological Sciences, Bond Life Sciences Center, Interdisciplinary Plant Group, and Missouri Maize Center, University of Missouri, Columbia, MO 65211-7310, USA
[3]Boron-Containing Functional Materials, Institute of Inorganic Chemistry and Institute for Sustainable Chemistry & Catalysis with Boron, University of Würzburg, Am Hubland, Würzburg 97074, Germany
[4]Institute of Organic Chemistry, University of Freiburg, Albertstr. 21, Freiburg im Breisgau 79104, Germany
[5]Chair of Plant Breeding, Technical University of Munich, Liesel-Beckman Str. 2, Freising 85354, Germany
[6]Institute of Crop Science and Resource Conservation, Plant Nutrition, University of Bonn, Karl-Robert-Kreiten Straße 13, Bonn 53115, Germany

*Author for correspondence: mmatthes@uni-bonn.de
[†]These authors contributed equally to the work.
The author responsible for distribution of materials integral to the findings presented in this article in accordance with the policy described in the Instructions for Authors (https://academic.oup.com/plphys/pages/General-Instructions) is M. Matthes.

Abstract

Both deficiency and toxicity of the micronutrient boron lead to severe reductions in crop yield. Despite this agricultural importance, the molecular basis underlying boron homeostasis in plants remains unclear. To identify molecular players involved in boron homeostasis in maize (*Zea mays* L.), we measured boron levels in the Goodman-Buckler association panel and performed genome-wide association studies. These analyses identified a *benzoxazinless* (*bx*) gene, *bx3*, involved in the biosynthesis of benzoxazinoids, such as 2,4-dihydroxy-7-methoxy-1,4-benzoxazin-3-one (DIMBOA), which are major defense compounds in maize. Genes involved in DIMBOA biosynthesis are all located in close proximity in the genome, and benzoxazinoid biosynthesis mutants, including *bx3*, are all DIMBOA deficient. We determined that leaves of the *bx3* mutant have a greater boron concentration than those of B73 control plants, which corresponded with enhanced leaf tip necrosis, a phenotype associated with boron toxicity. By contrast, other DIMBOA-deficient maize mutants did not show altered boron levels or the leaf tip necrosis phenotype, suggesting that boron is not associated with DIMBOA. Instead, our analyses suggest that the accumulation of boron is linked to the benzoxazinoid intermediates indolin-2-one (ION) and 3-hydroxy-ION. Therefore, our results connect boron homeostasis to the benzoxazinoid plant defense pathway through *bx3* and specific intermediates, rendering the benzoxazinoid biosynthesis pathway a potential target for crop improvement under inadequate boron conditions.

Introduction

The micronutrient boron is essential for proper plant growth (Warington 1923) and both deficiencies and toxicities of boron in the soil lead to severe yield reductions in many major crops, including maize (*Zea mays* L.) (Brdar-Jokanović 2020). Soils with either low or toxic boron levels are widespread in the world (Landi et al. 2019; Brdar-Jokanović 2020; and references therein), making the study of the effects of boron supply on plant development an important topic for agriculture. After uptake from the soil, boron moves along the transpiration stream and accumulates at its end. Consequently, excess boron accumulates at the leaf blade tips and extends into the margins (Brown and Shelp 1997; Marschner 2012), which causes leaf necrosis when boron supply is too high (Eaton 1944; Reid et al. 2004). Boron toxicity leads to reduced chlorophyll content, stomatal conductance, and photosynthesis (as reviewed in Landi et al. (2019)). Boron deficiency primarily affects meristematic tissues (Sommer and Sorokin 1928), leading to reductions in leaf blade width and length, sterility, and in severe cases to seedling lethality. In the root, both boron deficiency

and toxicity lead to a reduction in primary root length (Reid et al. 2004; Choi et al. 2007; Aquea et al. 2012; Esim et al. 2013; Poza-Viejo et al. 2018; Zhang et al. 2021) and to a reduction in lateral root density (Housh et al. 2020; Wilder et al. 2022). Understanding the molecular mechanisms that allow for efficiently using low levels or tolerating toxic levels of boron will help in developing efficient and tolerant varieties providing a sustainable solution to overcome yield reductions due to suboptimal or toxic boron supply.

The main characterized function of boron is in crosslinking of the pectin subunits rhamnogalacturonan-II (RG-II) in the cell wall (Kobayashi et al. 1996; Matoh et al. 1996; O'Neill et al. 1996) and boron efficiency processes include boron uptake, boron trans- and retranslocation, and boron utilization. From these processes, genetic components involved in boron uptake are currently best understood in the model organism *Arabidopsis thaliana* (Arabidopsis). Boron is taken up by plants in the form of boric acid and transported within plants in the form of the borate anion (for a recent review, see Onuh and Miwa (2021)). While passive uptake prevails in boron adequate soil conditions, facilitated

and active boron transport is needed in low and excess soil boron conditions. Boron transporters belong to the nodulin 26-like intrinsic protein (NIP) subfamily of the major intrinsic protein (MIP) family of boric acid importers and the high boron requiring family of borate exporters. In Arabidopsis, the 3 NIPs, involved in boron import, and the 7 BORs, involved in boron export, have tissue and functional specificities (as reviewed in Onuh and Miwa (2021)). The major players are AtNIP5;1 (Takano et al. 2006) and AtBOR1 (Noguchi et al. 1997). Orthologs of these genes have been characterized in many plant species, including maize (Chatterjee et al. 2014, 2017; Durbak et al. 2014; Leonard et al. 2014; Chatterjee et al. 2017). *Zmtassel-less1* (*Zmtls1*) is the *AtNIP5;1* co-ortholog in maize and shows seedling lethality, when grown in low boron conditions. When grown in adequate boron conditions, only reproductive defects are prominent (Durbak et al. 2014; Leonard et al. 2014). Due to impaired boron uptake, this mutant is inherently boron deficient in meristem tissues and all defects can be rescued by boron fertilization (Durbak et al. 2014; Matthes et al. 2018), making it a good tool to study boron deficiency responses in maize (Matthes et al. 2022, 2023). Boron transporters additionally were shown to provide molecular targets for engineering plants adapted to altered soil boron concentrations (Miwa et al. 2006; Sutton et al. 2007; Kato et al. 2009; Schnurbusch et al. 2010; Uraguchi et al. 2014; Hayes et al. 2015; He et al. 2021).

Several lines of evidence indicate that additional molecular candidates exist that either regulate intracellular levels of boron or adapt cellular metabolism to changing boron levels. For example, various classes of genes are differentially regulated in boron deficient and toxic conditions (Peng et al. 2012) and there are striking differences between phenotypes of boron transporter mutants and phenotypes of plants grown in boron-deficient conditions (as reviewed in Matthes et al. (2020)). Numerous studies additionally highlight the importance of meristem genes and phytohormone cascades in the adaptation of plants to low boron levels (Abreu et al. 2014; Eggert and von Wirén 2017; Poza-Viejo et al. 2018; Gómez-Soto et al. 2019; Matthes et al. 2022, 2023; Pommerrenig et al. 2022). Recently, the boron deficiency response was additionally shown to reflect a wounding response in *Brassica napus* (Verwaaijen et al. 2023). These examples suggest that there are additional pathways that regulate either plant boron levels or susceptibilities and therefore might be harnessed for developing high yielding crops in boron-deficient conditions.

In Arabidopsis, few non-boron transporter genes potentially involved in boron homeostasis were identified. Of those, specific transcription factors were identified that regulate boron import by directly binding to the promoter of the boron transporter gene *NIP5;1* (Kasajima and Fujiwara 2007; Kasajima et al. 2010; Feng et al. 2020; Zhang et al. 2024). For others, a link to boron transport remains elusive and they might therefore act independent of it. These include the *low boron tolerance 1* mutant (Huai et al. 2018), for which the underlying gene remains to be identified, and the *sensitive to high-level of boron 1* mutant, which is defective in *AtHEME OXYGENASE1*, involved in photomorphogenesis (Lv et al. 2017), genes encoding specific subunits of condensin II (Sakamoto et al. 2011), affecting RG-II biosynthesis or dimer formation (O'Neill et al. 2001; Sechet et al. 2018) or genes influencing the deposition of pectin in the cell wall (Hiroguchi et al. 2021). More recently evidence from Arabidopsis and *Rosa* cell suspension cultures emphasized the importance of a properly functioning Golgi apparatus for boron-related processes (Chormova et al. 2014; Chormova and Fry 2016; Begum and Fry 2022; Onuh and Miwa 2023).

Efforts to elucidate molecular mechanisms underlying boron homeostasis in crops are ongoing and include the assessment of genetic variation (Pommerrenig et al. 2018; He et al. 2021), quantitative trait locus (QTL) analyses (Paull et al. 1991; Jefferies et al. 1999, 2000; Xu et al. 2001; Sutton et al. 2007; Schnurbusch et al. 2010; Zhao et al. 2012; Pallotta et al. 2014), or genome-wide association studies (GWAS) (de Abreu Neto et al. 2017; Jia et al. 2021). Furthermore, transcriptome studies identified genes that respond to varying boron levels in the soil or growing media (Zeng et al. 2008). While such efforts detected various genomic regions and a multitude of genes affected by altered soil boron levels, the elucidation of molecular players instrumental for boron homeostasis, and therefore, deficiency or toxicity tolerance, is not resolved.

Here, we report the detection of the benzoxazinoid biosynthesis gene *benzoxazinless3* (*bx3*) as a molecular candidate associated with boron homeostasis in the major crop maize. Our study links altered boron levels with *bx3* and the benzoxazinoid pathway intermediates indolin-2-one (ION) and 3-hydroxy-indolin-2-one (HION). Benzoxazinoids are indole-derived secondary defense metabolites, which have best been studied in grasses (Poacea) and additionally independently evolved in some eudicot species (Florean et al. 2023). They not only regulate below and above-ground biotic interactions but are also known as signaling molecules and as iron chelators supporting iron uptake (Hu et al. 2018). Our study, therefore, adds another layer to the multifunctionality of benzoxazinoids and suggests the benzoxazinoid pathway as target for engineering plants adapted to altered soil boron concentrations.

Results

Goodman-Buckler association panel shows extensive variation in boron concentration in maize ear leaves

To investigate the extent of phenotypic variability of leaf boron concentrations, boron concentrations from 277 inbred lines (Supplementary Table S1) of the 282 maize Goodman-Buckler association panel (Flint-Garcia et al. 2005) were quantified. The diversity panel was grown in replicates in the summers of 2017 and 2018 at Genetics Farm of the University of Missouri, Columbia, USA, where soil boron concentrations of 0.39 mg/kg are considered low (Durbak et al. 2014; Matthes et al. 2018). This can be seen by the occurrence of the strong boron-deficient leaf phenotype of the maize *Zmtassel-less1* (*Zmtls1*) mutant, which is defective in active boron transport (Durbak et al. 2014; Matthes et al. 2022).

After flowering, the boron concentration of ear leaves (the leaf subtending the ear shoot) was analyzed. In the analyzed back-transformed best linear unbiased predictors (BLUPs) from the diversity panel, the boron concentration varied between 8.6 µg/g (line CMV3) and 17.8 µg/g (line IL14H) (Supplementary Table S1) with a mean of 11.9 µg/g (Supplementary Table S2). The broad sense heritability calculated on a line-mean basis was 0.31 (Supplementary Table S2), indicating that the boron concentration in maize ear leaves is a complex trait and warrants genetic dissection to unravel this complexity.

GWAS uncovers 2 significant loci associated with the natural variation in boron concentration

To associate the observed variation in ear leaf boron concentration with the diverse inbred lines in the Goodman-Buckler association panel, we performed a GWAS using BLUPs from the analyzed 277 inbred lines. Using the publicly available single nucleotide polymorphism (SNP) data from the 282 Goodman-Buckler association,

2 significant SNP-trait associations (Fig. 1A) were identified. One SNP was on chromosome 4 (chr4) and 1 on chr7 (Fig. 1A; Table 1), suggesting that the genomic regions that are in linkage disequilibrium (LD) with them were significantly associated with the ear leaf boron concentration in maize. A quantile-quantile plot from the GWAS showed that our GWAS model is not inflated and depicts that few *P*-values of the performed association tests between SNP data and boron concentration data were more significant than expected (Fig. 1B).

We identified 6 candidate genes from the 200 kb intervals (100 kb upstream and downstream) centered around the significant SNP on chr4 and 8 candidate genes centered around the SNP on chr7 (Table 1). Two of the 6 chr4 genes were annotated as *benzoxazinless3* (*bx3*) and *bx4* (Table 1), involved in benzoxazinoid biosynthesis. The annotated genes underlying the peak on chr7 encoded an alcohol dehydrogenase, a DNAJ domain-containing protein, and the gibberellin receptor GID1L2 (Table 1).

Correlation analysis of gene expression of GWAS hits and boron concentration in the Goodman-Buckler association panel

To assess a potential connection between the identified GWAS candidate genes' transcript expression and boron concentration in the maize ear leaf, a correlation analysis was performed using publicly available gene expression data of the GWAS candidate genes in leaf tissues of the 282 Goodman-Buckler association panel (Kremling dataset, Kremling et al. 2018; Supplementary Table S3). Of the 14 detected GWAS hits, data for 6 genes were available from the Kremling dataset. We detected significant
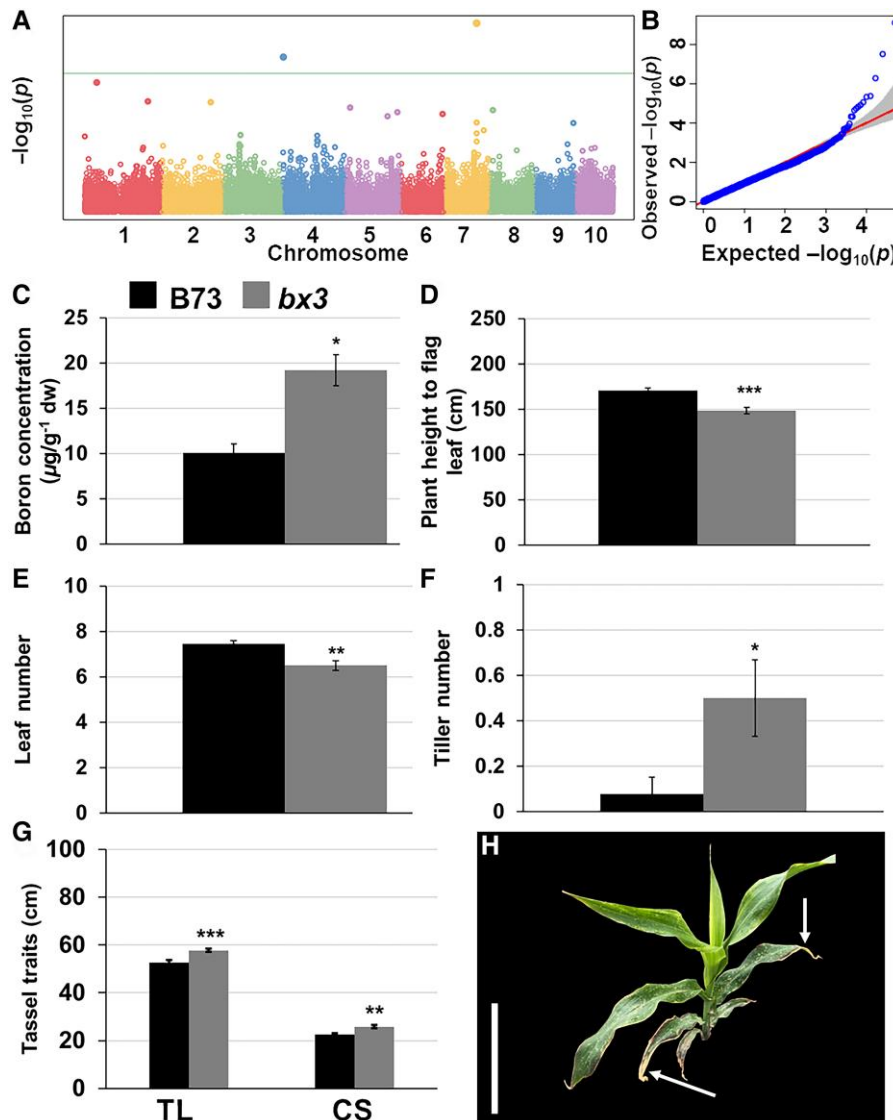

Figure 1. Phenotypes of the *bx3* mutant grown in the field (Bonn-Endenich 2020). **A)** Manhattan plot depicting genomic regions associated with variations of boron concentrations in a subset of the 282 Goodman-Buckler association panel. **B)** A quantile-quantile (qq) plot depicting the expected (*x*-axis) and observed (*y*-axis) −log(10) P-values. **C)** Boron concentration in ear leaves of the *bx3* mutant and B73 siblings. **D)** Plant height to flag leaf at maturity of the *bx3* mutant and B73 siblings. **E)** Leaf number between the leaf subtending the ear and the flag leaf of the *bx3* mutant and B73 siblings. **F)** Tiller number of the *bx3* mutant and B73 siblings. **G)** Tassel traits of the *bx3* mutant and B73 siblings. **H)** *bx3* plant image at 42 days after planting. The image was digitally extracted. Note that arrows in **H)** depicting leaf senescence at the leaf blade tip and the margins of *bx3*. Statistical analyses in **C)** through **G)** depict means and the error bars represent standard error of means. Sample numbers in **C to F)** were 13 (B73) and 14 (*bx3*) and in **G)** 10 (B73) and 11 (*bx3*). Statistical significance was calculated using Student's *t*-test (*P < 0.05, ***P < 0.005). Scale bar in **H)** = 15 cm. TL, tassel length; CS, length of central spike.

Table 1. GWAS of the boron concentration in ear leaves of the 282 Goodman-Buckler association panel and the candidate genes from 200 kb interval centered on the significant SNP (100 kb upstream/downstream) are summarized

Chr:SNP	Position	P-value	MAF	Effect size	Gene (B73_v2)	Gene (B73_v4) Zm00001d	Gene (B73_v5) Zm00001eb	Gene_description (v2)
4:ss196451184	3002213	3.34×10^{-08}	0.381	−0.011	GRMZM2G422877	48699	165520	Conserved gene of unknown function
					GRMZM5G896369	48701	165530, 165540	Hypothetical protein LOC100383896
					GRMZM5G830888, GRMZM2G469483	NA	NA	No description
					GRMZM2G167549	48702	165550	Cytochrome P450 71C2 (EC 1.14) (Protein benzoxazineless 3)
					GRMZM2G172491	48703	165560, 165570	Cytochrome P450 71C1 (EC 1.14) (Protein benzoxazineless 4)
7:ss196479729	126000000	7.81×10^{-10}	0.392	0.0124	GRMZM2G147191	20727	315020	Alcohol dehydrogenase
					GRMZM2G179045	20728	315030	Hypothetical protein LOC100381799
					GRMZM2G368058	20728	315030	No description
					GRMZM2G479068	20728	315030	No description
					GRMZM2G076802	NA	315040	DNAJ domain-containing protein
					GRMZM2G076778	20731	315050	Conserved gene of unknown function
					GRMZM2G003246	20732	315060	Gibberellin receptor GID1L2
					GRMZM2G518756	NA	NA	No description

Chromosome (Chr.), SNP ID, position, P-value, minor allele frequency (MAF), effect size, gene ID based on V2, V4, and V5 assembly, and gene description are summarized.

correlations between gene expression and boron concentration for 5 of the GWAS hits (*bx3* on chr4; alcohol dehydrogenase, DNAJ domain-containing protein, GRMZM2G076778 [which is a gene with unknown function], and Gibberellin Receptor on chr7) in one or multiple leaf tissues, suggesting that the variation of boron concentration in the Goodman-Buckler association panel might be correlated with expression level changes of these candidate genes. While *bx3* and the alcohol dehydrogenase gene showed a negative correlation in the third leaf, the DNAJ domain-containing protein and the Gibberellin Receptor genes showed positive correlations in various leaf tissues. GRMZM2G076778 depicted a negative correlation in adult leaf tissue (Supplementary Table S3).

The GWAS candidate genes *bx3* and *bx4* are differentially expressed in the maize boron transporter mutant *Zmtls1*

To further assess a connection between the identified genes and boron concentration in maize leaves, we tested, whether the identified GWAS candidate genes are differentially expressed in the maize boron transporter mutant *Zmtls1*, for which RNA-seq data of developing tassel meristems (~1 mm) are publicly available (Matthes et al. 2022). In *Zmtls1* tassel meristems, boron levels were found to be reduced compared with wild-type siblings (Durbak et al. 2014). We found that the chr4 candidate genes *bx3* and *bx4* were significantly upregulated in *Zmtls1* in that dataset, with log$_2$ fold changes of 1.56 for *bx3* (*P-adj* = 0.0013) and 1.42 for *bx4* (*P-adj* = 0.0025) (Matthes et al. 2022; Table 2). Notably, none of the other candidate genes on chr4 or chr7 appeared as differentially expressed in the *Zmtls1* RNA-seq dataset (Table 2).

Taken together, the chr4 candidate gene *bx3* was the only GWAS candidate, whose expression in leaf tissue (Kremling et al. 2018) showed a significant correlation with the measured leaf boron concentration in the 282 Goodman-Buckler association panel (negative correlation) and which was also differentially expressed in the boron-deficient tassel meristem of the *Zmtls1* mutant.

Mature plants of maize *bx3* mutants have a boron concentration phenotype

The previous GWAS and expression analyses linked the *bx3* gene with variation in boron concentration in maize. To test if there was a boron-associated phenotype in *bx3* mutants, we analyzed

Table 2. Differential expression of GWAS candidate genes and benzoxazinoid biosynthesis genes in developing meristems of Zmtls1 compared with wild-type controls

Gene ID	tls1 vs WT (log$_2$FC)	P-adj
Zm00001d048702 (*bx3*)	1.56	0.001288
Zm00001d048703 (*bx4*)	1.42	0.002502
Zm00001d48699 (unknown)		ns
Zm00001d48701 (hypothetical)		ns
Zm00001d20727 (alcohol dehydrogenase)		ns
Zm00001d20728 (hypothetical)		ns
Zm00001d20731 (unknown)		ns
Zm00001d20732 (gibberellin receptor GID1L2)		ns
Zm00001d048709 (*bx1*)		ns
Zm00001d048710 (*bx2*)		ns
Zm00001d048705 (*bx5*)		ns
Zm00001d048634 (*bx6*)	1.66	1.66×10^{-16}
Zm00001d049179 (*bx7*)		ns
Zm00001d048707 (*bx8*)		ns

ns, not statistically significantly different.

boron concentration in ear leaves of mature *bx3* mutants (Frey et al. 1997) and in the B73 inbred line grown at the field site in Bonn, where soil boron levels averaged 0.27 mg/kg. Soil boron concentrations in combination with the appearance of the strong seedling phenotype of the boron-deficient maize mutant *Zmtls1* in Bonn-Endenich (Supplementary Fig. S1) showed that these field site conditions are comparable to those at the Genetics Farm in Columbia, Missouri (Durbak et al. 2014), the field site used for the GWAS.

Analyses from field grown plants in 2020 and 2021 showed that boron concentration was significantly elevated in the ear leaves of *bx3* mutants compared with B73 (Fig. 1C; Supplementary Tables S2 and S3), substantiating a correlation between *bx3* and boron levels in maize. This increase was nutrient specific as the concentrations of the other tested micro- and macronutrients were either unchanged (magnesium, calcium, phosphorus, sulfur, iron, zinc) or even decreased (manganese, copper) in the *bx3* mutant. Only potassium also showed a mild increase in *bx3* ear leaves (Supplementary Table S4). During the 2023 field season, however, no elevated boron concentrations were detected in *bx3* ear leaves compared with B73 (Supplementary Fig. S1). Similar observations were made in the greenhouse, when *bx3* mutants were grown in boron-rich soil (ED73 soil boron = 1.97 mg/kg) (Supplementary Fig. S2). In addition, the *Zmtls1* phenotype was also less severe with enhanced boron concentrations in ear leaves under the 2023 field conditions and under greenhouse conditions (Supplementary Fig. S1). It, therefore, seems likely that either variation in soil boron concentration or additional, not yet identified environmental factors influenced the boron-related phenotype in *bx3* and *tls1*.

Elevated boron concentrations in *bx3* ear leaves compared with B73 siblings did not lead to striking differences in reported boron toxicity phenotypes, like leaf tip necrosis in mature leaves (Supplementary Figs. S2 and S3), suggesting that the elevated boron concentrations in *bx3* ear leaves were not toxic. However, earlier during vegetative development (42 days after planting [DAP] in the field), *bx3* mutants showed severe leaf senescence at the leaf blade tip of particularly older leaves, extending into the leaf blade margins, which was not observed in B73 (arrowed in Fig. 1H; Supplementary Fig. S3B), suggesting a developmental factor influencing the phenotypes observed in *bx3* mutants.

In addition, the *bx3* mutants showed minor alterations of other potentially boron-related phenotypes: Plant height (up to the flag leaf) was significantly reduced in *bx3* mutants compared with B73 (Fig. 1D), and *bx3* mutants had significantly fewer leaves between the ear and the tassel compared with B73 siblings (Fig. 1E). In addition, tiller number, tassel length (TL), and the length of central spike (CS) were significantly increased in *bx3* mutants compared with B73 siblings (Fig. 1, F and G; Supplementary Table S5). While kernel row number was slightly, but significantly reduced in *bx3* mutants compared with B73 control plants, ear length was significantly longer (Supplementary Table S5). These morphological data suggested that enhanced boron levels in the *bx3* mutants did not lead to striking boron toxicity symptoms in field grown plants at maturity.

Bx3 mutants show a leaf tip necrosis phenotype during seedling development and its severity correlates with boron levels

In order to characterize the impact of boron levels on the observed leaf tip necrosis phenotype that we observed 6 weeks after planting (Fig. 1H), we analyzed the phenotype of *bx3* mutants earlier in development grown with different levels of boron. We first grew

bx3 mutants and B73 siblings in the growth chamber in boron sufficient soil (boron concentration of ED73 soil = 1.97 mg/kg) and phenotypically characterized seedling development over time (Fig. 2; Supplementary Table S6). We evaluated plant height, V-stage, leaf tip necrosis, and leaf number at 14 (developmental stage: V1/2 with 3 to 4 leaves emerged) and 25 DAP (developmental stage: V3/4, with 5 to 6 leaves emerged) (Fig. 2; Supplementary Fig. 4G and Table S6). At both time points, the *bx3* mutant was phenotypically not distinguishable from B73 with respect to plant height, leaf number, and V-Stage (Supplementary Table S6). However, at 14 DAP (developmental stage: V1/2), when both B73 and *bx3* had 3 to 4 leaves, the leaf tips of leaves 1 and 2 showed a distinct leaf tip necrosis phenotype in *bx3* mutants, but not in the B73 control (Fig. 2, A to C). In addition, we detected statistically significantly higher boron concentrations in pooled first and second leaves of *bx3* mutants compared with those of B73 14 DAP (Fig. 2D). This showed that boron levels are also enhanced in seedling leaves of the *bx3* mutant and suggested that these elevated boron levels correlated with the observed leaf tip necrosis phenotype.

Since the *Zmtls1* mutant showed enhanced boron levels in ear leaves under field conditions in 2023 (Supplementary Fig. S1), we did not use a genetics approach using double mutant analysis to determine the effects of lowered boron levels on *bx3* mutants. Instead, we grew the *bx3* mutants and B73 control plants in boron-free media (HGoTech GmbH, Bonn, Germany), where boron concentration = 0.03 mg/kg.

The leaf tip necrosis phenotype remained present in the *bx3* mutant, when grown in the boron-free media, whereas boron concentration in seedling leaves of *bx3* (leaves 1 and 2 pooled) were not statistically significantly different from the B73 control (Fig. 2, E to H). Therefore, we tested whether adding extra boron could influence the severity of the leaf tip necrosis phenotype by subjecting *bx3* mutants and B73 control plants (grown in ED73 soil) to the following watering regimes: Ultra-pure water (Merck Millipore, Burlington, USA), Peter's fertilizer (ICL specialty fertilizers, Tel-Aviv, Israel), Peter's fertilizer +0.5 mM boric acid, and Peter's fertilizer +1 mM boric acid. The ultra-pure water and Peter's fertilizer treatments showed the leaf tip necrosis phenotype in *bx3* plants, but not in B73 plants 14 DAP. In contrast, the treatments with Peter's fertilizer and additional boric acid caused the occurrence of the leaf tip necrosis phenotype also in B73 seedlings (Fig. 3, A to C; Supplementary Table S7), suggesting that the additional boric acid treatment caused this phenotype even in B73. In the *bx3* mutant, no enhancement of the leaf tip necrosis score was detected between the different watering regimes; however, the senesced leaf area in *bx3* mutants was significantly larger in the additional boric acid treatments compared with the ultra-pure water and Peter's fertilizer treatments (Fig. 3D).

Taken together, these analyses showed that the severity of the leaf tip necrosis phenotype in *bx3* mutants is correlated with enhanced boron levels. However, the variability of the results indicated that there are also additional, so far unidentified factors, contributing to the leaf tip necrosis phenotype in *bx3* mutants.

Investigation of a correlation between additional benzoxazinoid pathway genes and boron homeostasis

To determine if the link between boron levels and *bx3* was specific to *bx3*, we investigated other genes in the benzoxazinoid pathway. *bx3* encodes a cytochrome P450 monooxygenase that is involved in the biosynthesis of benzoxazinoids, a group of specialized secondary metabolites (Frey et al. 1997; Supplementary Fig. S5). The
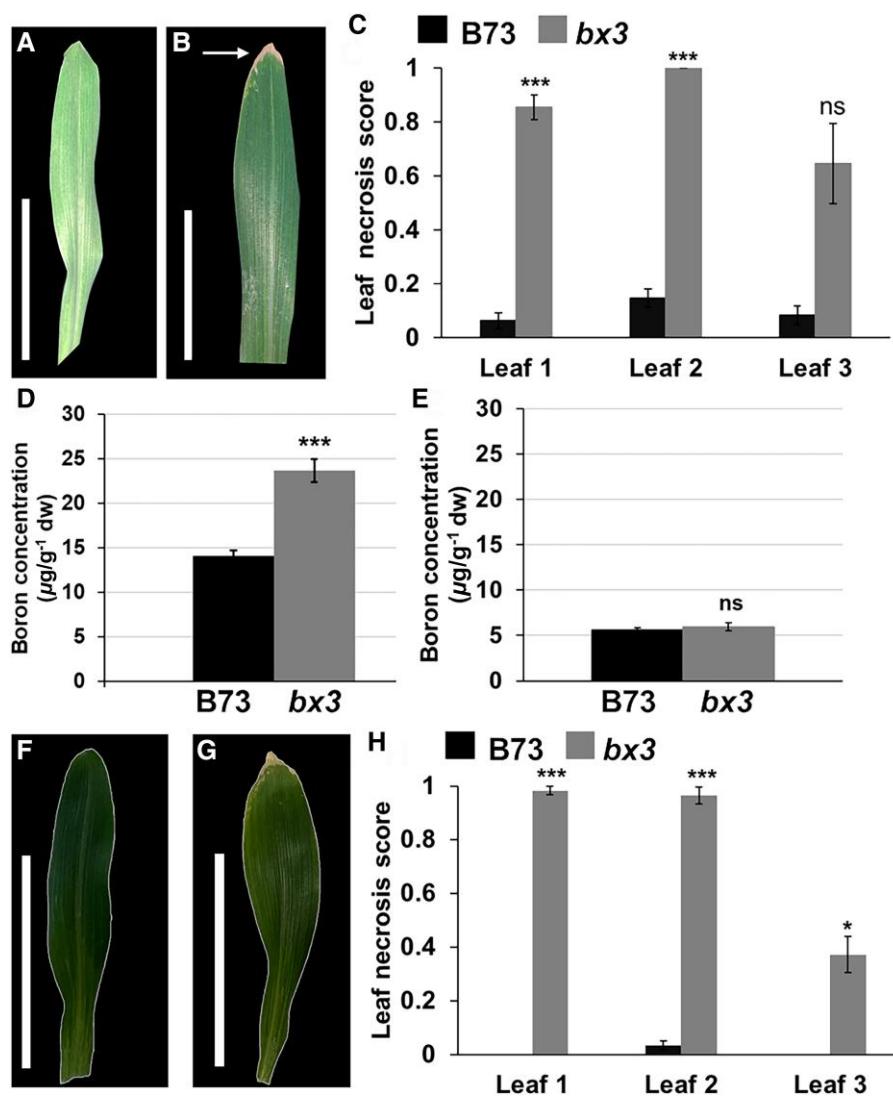
Figure 2. Leaf phenotypes of B73 and *bx3* seedlings. Images of the first leaves of **A)** B73 and **B)** *bx3* 14 days after planting (DAP) grown in the growth chamber in ED73 soil (boron concentration = 1.97 mg/kg). Arrows indicate leaf tip senescence. The images were digitally extracted for comparison. **C)** Statistical analysis of leaf tip necrosis in all emerged leaves of ED73-grown B73 and *bx3* 14 DAP. Depicted are means of 3 biological replicates, where *n* = 16 per genotype and biological replicate. Error bars show standard error of means. Statistical analysis of boron concentration (μg/g dw) in leaves 1 and 2 (pooled) of B73 and *bx3* 14 DAP, when **D)** seedlings grew in ED73 soil and **E)** seedlings grew in HGoTech substrate (boron concentration 0.03 mg/kg). Given are means over 4 biological replicates. The error bars represent standard error of means. Images of the first leaves of **F)** B73 and **G)** *bx3* 14 DAP grown in the growth chamber in HGoTech substrate. Images are digitally extracted for comparison. **H)** Statistical analysis of leaf tip necrosis in all emerged leaves of HGoTech-grown B73 and *bx3* 14 DAP. Depicted are means of 4 biological replicates, where *n* = 15 per genotype and biological replicate. Error bars show standard error of means. Statistical significance in **C)**, **D)**, and **H)** at *$P < 0.05$, **$P < 0.01$, ***$P < 0.005$ according to Student's *t*-test. Scale bars in **A, B, and F)**, **G)** = 5 cm. ns, not statistically significantly different.

predominant benzoxazinoids are 2,4-dihydroxy-1,4-benzoxazin-3-one (DIBOA) and 2,4-dihydroxy-7-methoxy-1,4-benzoxazin-3-one (DIMBOA), the latter being the major benzoxazinoid in B73 maize. There are 14 characterized *bx* genes in maize (as reviewed in de Bruijn et al. (2018)) with *bx1* to *bx9* involved in the synthesis of DIMBOA and *bx1* to *bx8* being located in proximity on chr4 (as reviewed in Frey et al. (2009)). We, therefore, assessed the possibility that the GWAS detected a significant correlation with the *bx* gene cluster on chr4, rather than individual *bx* genes, which was also reasoned by the detection of both *bx3* and *bx4* in the GWAS (Table 1). We performed correlation analyses with publicly available expression data in leaf tissue (Kremling et al. 2018) for all *bx* genes located on chr4 and the boron concentration data obtained from 277 lines of the 282 Goodman-Buckler association panel (Supplementary Table S1), similar to the correlation analyses with the detected

GWAS candidates (Supplementary Table S3). These analyses showed that, in addition to gene expression of *bx3*, that of *bx2* also showed a negative correlation in the base of third leaf tissue, and that of *bx5* showed a positive correlation in the tip of third leaf tissue with boron concentration (Supplementary Table S8).

Furthermore, we examined *bx* gene expression of the chr4 cluster in the developing tassel meristem dataset of the *Zmtls1* mutant, which has reduced boron levels in that tissue. We found that in addition to *bx3* and *bx4*, also expression of *bx6* is significantly upregulated in *Zmtls1* mutants compared with normal siblings (Table 2). These results indicated that a potential correlation between *bx* genes and boron concentration in maize might not be restricted to *bx3* and that benzoxazinoid biosynthesis could be altered in *Zmtls1*. Therefore, we quantified levels of DIMBOA in *Zmtls1* leaves and found that the levels were significantly reduced
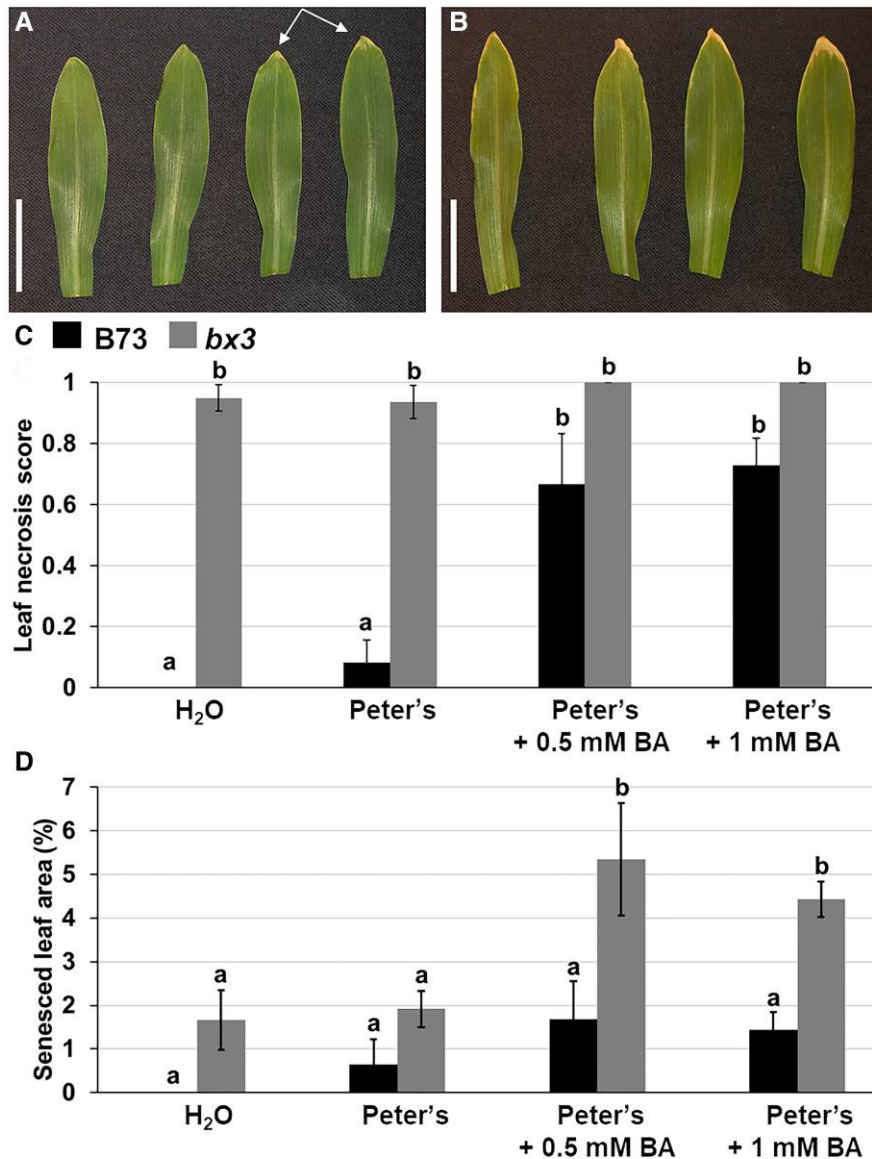
Figure 3. Senesced leaf area is enhanced by boron fertilization. Images of first leaves of **A)** B73 and **B)** *bx3* grown in ED73 soil. The images were taken 14 days after planting (DAP) with different watering regimes (from left to right: H_2O, Peter's fertilizer, Peter's fertilizer +0.5 mM boric acid (BA), Peter's fertilizer +1 mM BA). Arrows in **A)** point to leaf tip necrosis in B73. **C)** Statistical analysis of leaf necrosis score 14 DAP in B73 and *bx3* seedlings. **D)** Statistical analysis of senesced leaf area 14 DAP in B73 and *bx3* seedlings. **C and D)** show means of 4 biological replicates with 4–6 individuals per genotype and replicate. Error bars represent standard error of means. Different letters indicate statistical significance at $P < 0.05$ according to an analysis of variance with post hoc multiple comparison correction using the Tukey algorithm.

compared with wild-type controls (WT = 462.01 ± 71.01 ng/g, *Zmtls1* = 229.41 ± 59.99 ng/g, $P < 0.05$).

Boron homeostasis appears to be linked to *bx3* rather than DIMBOA

To test potential correlations between boron levels and benzoxazinoid biosynthesis, we analyzed boron concentration and assessed the leaf tip necrosis phenotype in *bx1* and *bx2* mutants, which were reported to have reduced DIMBOA levels (Hamilton 1964; Frey et al. 1997; Tzin et al. 2015).

We found that boron levels in ear leaves of *bx1* or *bx2* mutants were not statistically significantly different compared with their respective inbred control (Fig. 4A), when grown in Bonn-Endenich (soil boron concentration: 0.27 mg/kg in 2021). Likewise, *bx1* (developmental stage: V1/2) and *bx2* mutants (VE/1) did not show the

striking leaf tip necrosis phenotype observed in *bx3* mutants (developmental stage: V1/2) at 14 DAP (Fig. 4, B to E, Supplementary Table S9). While the *bx2* mutant (introgressed in W22 and not B73) was not at the same developmental stage (VE/1) as *bx1* or *bx3* at 14 DAP, it did not show a statistically significant difference in leaf tip necrosis compared with its inbred control (W22) in any of the analyzed timepoints (Supplementary Table S9). In contrast, *bx1* showed a similar leaf tip necrosis phenotype to *bx3* at 18 DAP (developmental stage of both mutants: V2) and at 25 DAP (developmental stage of both mutants: V3). This phenotype, however, was restricted to the first leaf (18 DAP) or the first 2 leaves (25 DAP) (Fig. 4; Supplementary Table S9), which was in contrast to *bx3*, where the leaf necrosis phenotype was present in all developed leaves (Supplementary Table S9).

Taken together, our analyses therefore suggested a link between boron and *bx3* rather than boron and DIMBOA and raised
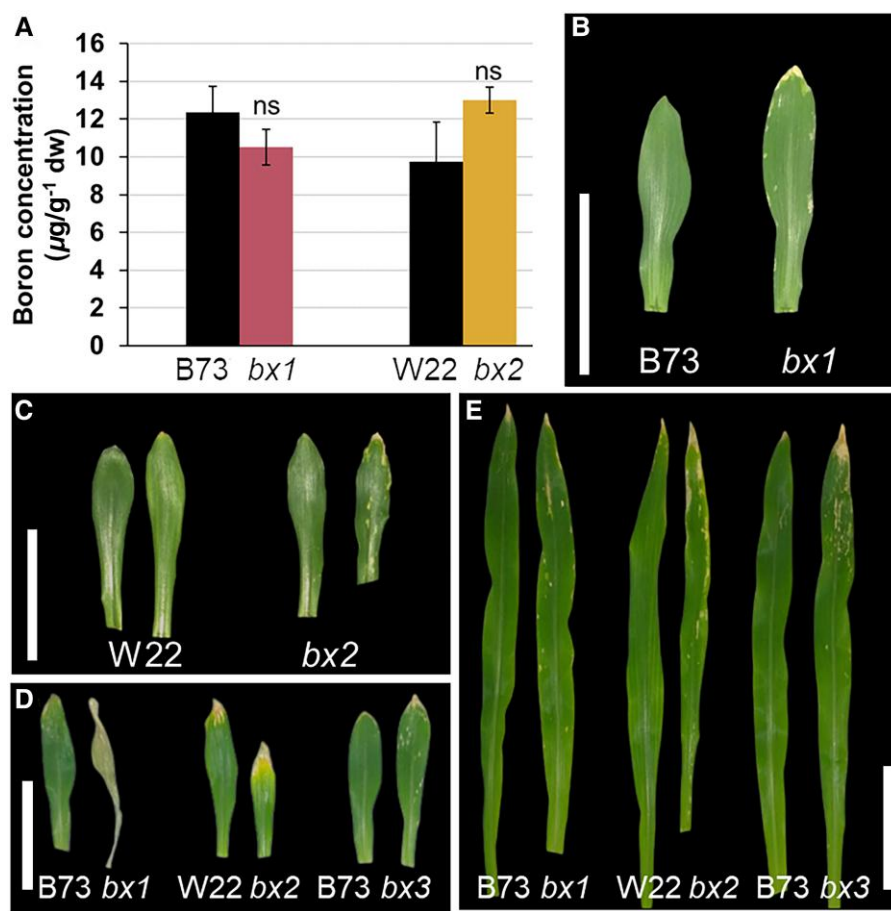
Figure 4. Boron-related phenotypes observed in the *bx3* mutant are not found in *bx1* or *bx2*. **A)** Statistical analysis of boron concentration (µg/g) in ear leaves of *bx1* and *bx2* mutants compared with the respective inbred control (grown in the field, Bonn-Endenich). Depicted are means ± standard error of means and statistical significance was calculated using Student's *t*-test ($P < 0.05$) ($n = 3$, where each replicate is a pool of four individual leaves). Leaf phenotypes of B73, W22, and mutants of *bx1*, *bx2*, *bx3* at 14, 18, and 25 days after planting (DAP), where **B)** Leaf 1 at 18 DAP, **C)** Leaf 1 at 18 DAP, **D)** Leaf 1 at 25 DAP, **E)** Leaf 2 at 25 DAP. The images in **B to E)** were digitally extracted. Scale bars in **B to E)** = 5 cm.

the question whether the lack of a functional BX3 enzyme or the accumulation of the BX3 substrate (Supplementary Fig. S5A) is connected with the observed boron accumulation.

Boron concentration is elevated in transgenic Arabidopsis lines expressing *BX1* and *BX2*

Although all 3 maize *bx* mutants we investigated are DIMBOA deficient (Frey et al. 1997; Tzin et al. 2017), *bx3* unlike *bx1* and likely *bx2* also accumulates the intermediate ION, which is the substrate of the BX3 enzyme (Abramov et al. 2021; Supplementary Fig. S5A). In order to test, whether elevated ION levels correlate with the observed boron concentration elevation in the *bx3* mutant, we made use of Arabidopsis lines, where parts of the benzoxazinoid biosynthesis pathway were transgenically introduced (Abramov et al. 2021). Arabidopsis does not endogenously express this pathway, allowing an assessment of a potential boron–benzoxazinoid correlation in a "clean" background. We found that boron concentration in rosette leaves at bolting stage of *pSUR2::Bx1Bx2*, which accumulate ION, was significantly higher compared with the *Col-0* control. On the other hand, functional expression of BX3 (*p35S::Bx3* lines, which do not accumulate ION) did not influence the boron concentration. Therefore, a direct effect of the enzyme seems to be unlikely (Fig. 5). In addition, *pSUR2::Bx1Bx2* overexpressing lines showed a subtle leaf tip necrosis phenotype, compared with *Col-0* and *p35S::Bx3* lines (Fig. 5). Since *pSUR2::BX1BX2*

lines were reported to additionally show elevated salicylic acid (SA) levels, we additionally assessed the impact of SA accumulation on the boron-related phenotypes of *pSUR2::Bx1Bx2* lines, by analyzing *pSUR2::Bx1Bx2* crossed to *NahG* lines (*pSUR2::Bx1Bx2 x NahG*), where the SA hydroxlase *NahG* was introduced (Abramov et al. 2021). Our results showed that boron concentration is also significantly elevated in *pSUR2::Bx1Bx2xNahG* rosette leaves compared with *Col-0* controls and that the leaf tip necrosis phenotype in these lines is enhanced (Fig. 5, E and F; Supplementary Table S10). Therefore, these results suggested that a correlation between boron levels and the benzoxazinoid pathway is linked to an accumulation of the intermediate ION.

Boric acid forms a complex with the benzoxazinoid intermediate 3-hydroxy-ION (HION)

The benzoxazinoid DIMBOA was reported to chelate iron thus making it bioavailable (Hu et al. 2018), but also complex formation between DIMBOA and other nutrients, including zinc, copper, and manganese was reported (as reviewed in Wouters et al. (2016)). We therefore reasoned that elevated boron levels in the *bx3* mutant could be related to a benzoxazinoid-mediated alteration of boron transport or mobility. The correlation between boron levels and an accumulation of ION led us to test the hypothesis that boric acid and ION might form a complex, which in turn might
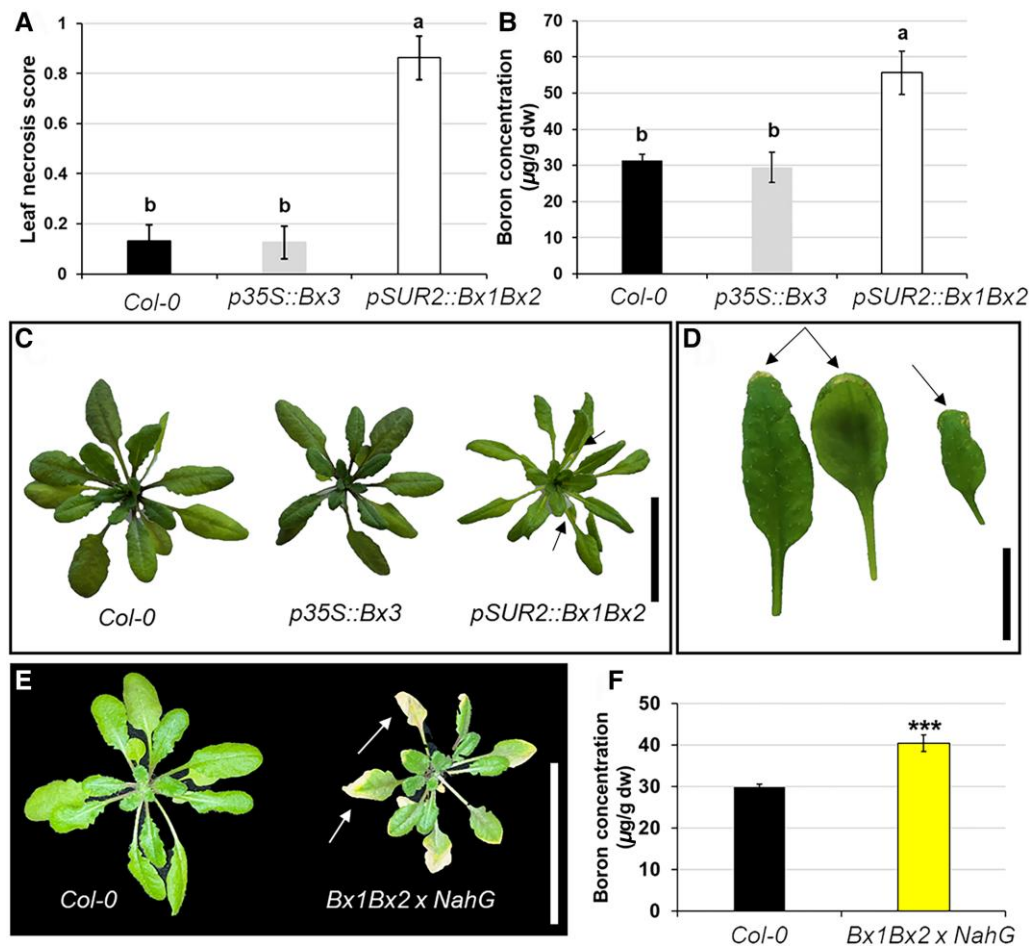
Figure 5. Analysis of boron–benzoxazinoid relations in transgenic Arabidopsis. **A)** Statistical analysis of leaf tip necrosis in *Col-0*, *p35S::Bx3*, and *pSUR2:: Bx1Bx2* Arabidopsis lines. **B)** Statistical analysis of boron concentration (µg/g dw) in *Col-0*, *p35S::Bx3*, and *pSUR2::Bx1Bx2* Arabidopsis lines. **C)** Rosette leaf phenotypes of *Col-0*, *p35S::Bx3*, and *pSUR2::Bx1Bx2*. Note that arrows in *pSUR2::Bx1Bx2* pointing to a leaf tip necrosis phenotype in older leaves. **D)** Images of different leaves showing a subtle leaf tip necrosis phenotype in *pSUR2::Bx1Bx2* transgenic Arabidopsis. Note arrows that point to the leaf tip necrosis phenotype. **E)** Rosette leaf phenotypes of *Col-0* and *pSUR2::Bx1Bx2* in the *NahG* mutant background (*pSUR2::Bx1Bx2xNahG*). Note arrows in *pSUR2:: Bx1Bx2xNahG* pointing to severely senesced rosette leaves. The images in **C to E)** were digitally extracted for comparison. **F)** Statistical analysis of boron concentration (µg/g dw) in *Col-0* and *pSUR2::Bx1Bx2xNahG* Arabidopsis lines. Statistical analyses in **A, B, and F)** depict means over 3 to 4 biological replicates ($n = 13$–15 individuals per biological replicate) ± standard error of means. Different letters indicate statistically significant differences according to an analysis of variance and post hoc Tukey test ($P < 0.05$). *** indicates statistical significance at $P < 0.005$ according to Student's *t*-test. Scale bars in **C)** = 4.5 cm, in **D)** = 1 cm, and in **E)** = 5 cm.

influence boron transport or mobility in maize. The reaction between ION and boric acid, however, did not lead to any boric acid–ION complex (Supplementary Fig. S6). As boron is known to specifically interact with *cis*-diol groups, which are not present in the benzoxazinoid intermediate ION, we also tested the next intermediate in the benzoxazinoid pathway, 3-hydroxy-ION (HION). HION is the product of the enzymatic function of BX3 (Supplementary Fig. S5A) that may tautomerize to the lactim species bearing 2 *cis*-diol groups (Supplementary Fig. S5B). The reaction of HION with boric acid in the presence of a base led to numerous additional signals in the ^{11}B-NMR spectrum (Fig. 6A) and ^{1}H-NMR spectrum (Supplementary Fig. S7A). Importantly, these signals were not observed when the analysis was done with boric acid and base alone (Fig. 6B) or when the control experiments were performed in the absence of boric acid (Supplementary Fig. S7, B and C). These results suggested the formation and therefore the existence of additional boron compounds formed between boric acid and HION (Fig. 6). Attempts to identify the nature of these additional boron compounds were unsuccessful, suggesting that such a complex is unstable. In the presence of air, HION reacted

to isatin, which was not dependent on the presence of boric acid (Supplementary Fig. S6).

Discussion

Identification of genomic loci involved in boron homeostasis in maize

Previous analyses of genetic variation in various plant species that detected QTLs or genomic regions associated with boron deficiency or toxicity tolerance, identified mostly boron transporter-related genes (Sutton et al. 2007; Zeng et al. 2008; Schnurbusch et al. 2010; Pallotta et al. 2014; Pommerrenig et al. 2018; He et al. 2021; Jia et al. 2021). Notably, the significantly associated SNPs on chr4 and chr7 in the GWAS analysis did not harbor any of the published boron transporter genes in maize, which are located on chr1 (*Zmtls1* and *Zmrte*) and on chr3 (*Zmrte2*) (Chatterjee et al. 2014, 2017; Durbak et al. 2014; Leonard et al. 2014). It is likely that passive, protein-independent boron transport was still prevailing in the low boron field conditions, therefore masking any potential influence of active or facilitated boron transporters.
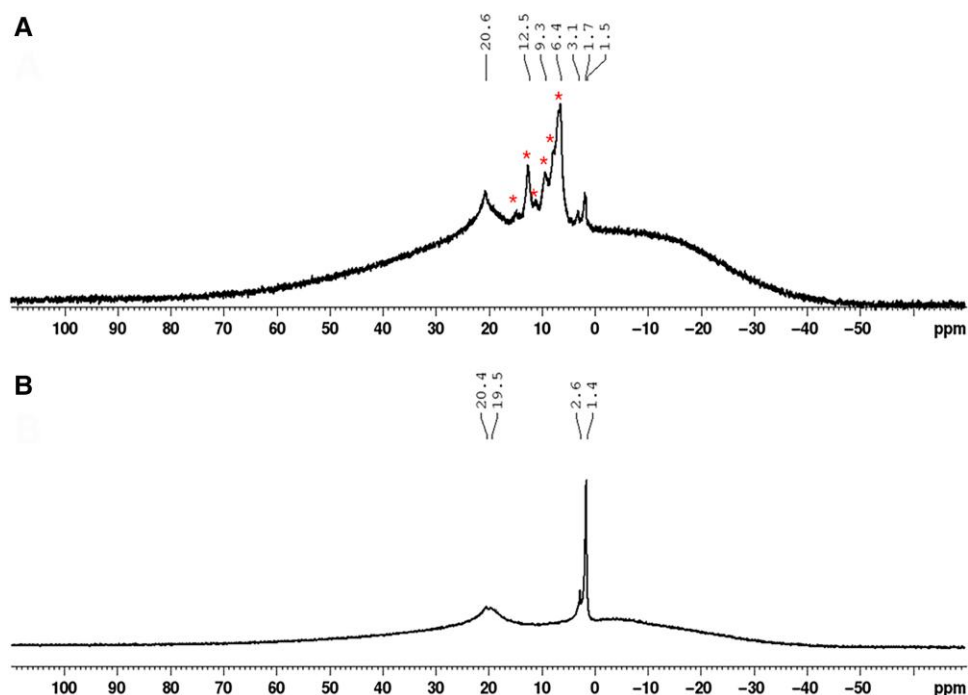
Figure 6. Boric acid reacts with HION to form additional boron species. **A)** The ^{11}B-NMR spectra showing the crude product of the reaction between HION and boric acid in the presence of a base and **B)** the crude product of the control experiment performed in the absence of HION. Signals assigned to the additional species are marked with an asterisk.

Similar studies using boron concentrations from seed as input have either detected specific boron transporters, like *Zmrte2* (Wu et al. 2021) and uncharacterized genes in maize (Schaefer et al. 2018) or peanut (Zhang et al. 2019), highlighting the potential contribution of non-boron transporter-related genes regulating boron homeostasis in plants.

Studies in rice, barley, and peanut have detected various cytochrome P450 proteins (with unknown function or putative iron-binding function) to be associated with either boron efficiency traits or boron concentration (Hassan et al. 2010; de Abreu Neto et al. 2017; Zhang et al. 2019), yet *bx* genes, which encode substrate specific cytochrome P450 proteins in grasses, have to our knowledge not been detected as potential candidates influencing boron-related processes in plants previously. Our study suggests that particularly *bx3* represents a molecular player associated with boron homeostasis in maize.

While we did not further test the additional GWAS hits detected (Table 1), the identification of a gene encoding a gibberellin receptor GID1L2 (GRMZM2G003246) on chr7 is worth mentioning. A functional role of gibberellin signaling in shaping the maize ionome had been suggested before (Schaefer et al. 2018) and it seems possible that gibberellin signaling or perception might be involved in boron concentration variation. Indeed, a rice GWAS analysis for boron toxicity tolerance also detected a gibberellin receptor (de Abreu Neto et al. 2017), providing evidence for the aforementioned hypothesis and for the applicability of our approach to detect molecular players involved in boron homeostasis. In addition, this finding adds to the importance of phytohormones in the boron response of plants (Martín-Rejano et al. 2011; Abreu et al. 2014; Camacho-Cristóbal et al. 2015; Li et al. 2015; Matthes and Torres-Ruiz 2016; Eggert and von Wirén 2017; Poza-Viejo et al. 2018; Gómez-Soto et al. 2019; Zhang et al. 2021; Matthes et al. 2022, 2023; Pommerrenig et al. 2022) and complements the reports of connections between the adaptation of plants to low or excess

boron and gibberellins (Alva et al. 2015; Eggert and von Wirén 2017).

The unprecedented association between the benzoxazinoid pathway and boron levels is a surprising discovery, particularly because it suggests *bx3* as a non-boron transporter-related gene associated with boron homeostasis in maize. We detected reduced DIMBOA levels and upregulation of various *bx* biosynthesis genes in the boron transporter mutant *Zmtls1* (Table 2), which corroborates previous results showing a transcriptional feedback inhibition of benzoxazinoid biosynthesis genes by DIMBOA (Ahmad et al. 2011). However, altered boron levels and the leaf tip necrosis phenotypes were most pronounced in *bx3* mutants, compared with *bx1* or *bx2* mutants, although all 3 mutants have reduced DIMBOA levels. Besides a reduction of DIMBOA, the *bx3* mutant, unlike *bx1* or *bx2* mutants, was reported to accumulate the intermediate ION (Abramov et al. 2021). Since the benzoxazinoid pathway is blocked from ION on in the *bx3* mutant, it can be assumed that not just DIMBOA but also the direct product of BX3, namely HION, is depleted in the *bx3* mutant. Therefore, a depletion of HION or a shift in the ION to HION ratio might be of greater importance for the observed boron-related phenotypes than reduced DIMBOA levels in the *bx3* mutant. This makes it tempting to speculate about a causal connection between these intermediates (ION and/or HION) rather than DIMBOA and enhanced boron levels in the *bx3* mutant. This hypothesis is supported by the finding that transgenic Arabidopsis lines, that overexpress *bx1* and *bx2* and therefore accumulate ION (Abramov et al. 2021), also showed elevated boron levels in rosette leaves and a leaf tip necrosis phenotype (Fig. 5), similar to what was observed in the maize *bx3* mutant (Figs. 1 and 2). In the transgenic Arabidopsis lines, ION was further shown to be hydroxylated and glucosylated by endogenous Arabidopsis enzymes to yield the metabolite, indoline-2-one-5-β-D-glucopyranoside (5HIONG; Abramov et al. 2021). Therefore, the Arabidopsis boron-related phenotypes might

not just be connected to enhanced ION levels, but also to different intermediates/metabolites, like 5HIONG and/or ratio shifts of ION to such additional metabolites. Furthermore, the detection of additional boron species using ^{11}B-NMR and ^{1}H-NMR analyses of HION and boric acid mixtures (Fig. 6) provide compelling evidence for the ability of HION to form a complex with boric acid. While the identity of the additional boron species and proof for such a complex *in planta* remains elusive, it is tempting to speculate that a mechanistic link between boron levels and the benzoxazinoid pathway might be connected to the formation of boron–benzoxazinoid complexes, hence affecting boron homeostasis. While this remains intriguing and speculative the association of boron-related processes with the benzoxazinoid pathway opens up exciting lines of research in both areas.

Elevated boron levels toxic, beneficial, or both?

The *bx3* mutant, grown in low boron field conditions, showed elevated boron concentrations in the ear leaves, yet boron toxicity phenotypes were subtle at maturity (reduced plant height, increased tillering) (Fig. 1; Supplementary Fig. S3), suggesting that the enhanced boron levels were not high enough to be detrimental to plant performance. On the contrary, strong leaf senescence phenotypes were observed at the seedling stage (Figs. 1H and 2), indicating that elevated boron levels are more detrimental during juvenile vegetative development, although there are also additional factors that contribute to the leaf senescence phenotype (Fig. 2; Supplementary Fig. S3). Boron requirements are higher during reproductive development compared with vegetative development in maize (Lordkaew et al. 2011; Durbak et al. 2014) and *bx* gene expression is higher during seedling development (Frey et al. 1995, 1997), providing explanations for the leaf senescence phenotype observed in *bx3* seedlings, but not in mature plants. Since boron soil levels at the field site in Bonn-Endenich can be considered low (soil boron concentration: 0.27 mg/kg), it seems possible that the enhanced boron concentration in *bx3* mutants at maturity might counteract soil induced boron deficiency in contrast to provoking toxicity symptoms. This hypothesis is supported by the finding that specific tassel traits, like TL and length of CS, but also ear traits, like ear length, were significantly longer in *bx3* compared with B73 plants (Fig. 1G; Supplementary Table S5). This observation further complements published results, showing that boron supplementation increases tassel and ear size (Durbak et al. 2014; Leonard et al. 2014; Matthes et al. 2018). Our findings, therefore, allow a future assessment of *bx3* and potentially other *bx* genes as suitable molecular candidates for the adaptation of maize to low boron soil conditions.

Conclusion

Understanding the molecular regulation of boron homeostasis in crops remains a challenging task. By using a GWAS approach in combination with mutant and chemical analyses, we showed that the benzoxazinoid pathway is linked to boron homeostasis likely through *bx3* and the pathway intermediates ION and HION.

Materials and methods
Germplasm and plant growing conditions

In total, 277 inbred lines of the 282 Goodman-Buckler association panel (Flint-Garcia et al. 2005), consisting of diverse maize (*Zea mays* L.) lines including tropical, sub-tropical, temperate, sweet corn, and popcorn lines, were grown in a randomized complete

block design in the summers of 2017 and 2018 at Genetics Farm of the University of Missouri (Columbia, Missouri, USA). Soil boron concentration in both years was 0.39 mg/kg as evaluated with the azomethine H method (Lohse 1982) by the Soil and Plant Testing Laboratory of the University of Missouri, which can be considered low considering the recommendation to apply boron to field maize, when soil levels are <0.75 ppm (Heckmann 2009).

The alleles used for the respective mutants were *Bx3::Mu* (*bx3*) (Frey et al. 1997), *bx1::Mu* (*bx1*) (Frey et al. 1997), *bx2::Ds* (*bx2*) (Tzin et al. 2017), and *tls1-ref* (*tls1*) (Durbak et al. 2014). The *bx1*, *bx3*, and *tls1* mutants were backcrossed at least 3 times to B73. Homozygous wild-types (B73) originating from the individual lines were used as controls. The *bx2* mutants were in a1-m3 background in the W22 inbred line, and the corresponding a1-m3 wild-type, also in the W22 background, was used as control. The *bx2* mutants and the corresponding wild-type (W22) were obtained from Dr. Georg Jander and Kevin Ahern (Boyce Thompson Institute, USA). In homozygous *bx3* plants, no DIMBOA can be detected and therefore can be considered null mutants (Frey et al. 1997). Homozygous *bx3* mutants from segregating lines were selected through genotyping using bx3_+540_F (5′-CAC CAA GAA GGT GCA GTC CT-3′), bx3_+1144_R (5′-GTA GCT GGA CTT ACC ACC AAG A-3′), and TIR6 (5′-AGA GAA GCC AAC GCC AWC GCC TCY ATT TCG TC-3′) primers. Genotyping for *tls1* was done as previously described (Durbak et al. 2014).

Unless otherwise stated, all maize greenhouse and growth chamber experiments were done with ED73 soil (Einheitserdewerke Werkverband e.V., Sinntal-Altengronau, Germany).

The transgenic Arabidopsis (*Arabidopsis thaliana*) lines, overexpressing parts of the maize benzoxazinoid pathway, namely *pSUR2::Bx1Bx2*, *pSUR2::Bx1Bx2xNahG*, and *p35S::Bx3* are described in Abramov et al. (2021). Seeds of the transgenic lines and the *Col-0* control were sown on 1% H_2O Agarose plates and stratified for 4 d at 4 °C in the dark. Afterwards, seeds were allowed to germinate for 7 d under long day conditions (light: 16 h, 22 °C, dark: 8 h, 17 °C, 40% humidity, light intensity = 65 $\mu E/m^2$/s), before seedlings were transferred to soil (Floragard B fein, sand, Perligran G mix, 10:1:1).

Boron concentration measurements

For the GWAS experiment in total, 277 inbred lines of the Goodman-Buckler association panel (Flint-Garcia et al. 2005) were used. In 2017 and 2018, leaves from the node subtending the ear shoot (referred to as ear leaves) from 5 plants per inbred line were collected after flowering, pooled, and about 2 cm of the leaves from the tip were discarded. The remaining leaf blades were dried at 60 °C and ground to a fine powder. Boron concentration in individual lines was analyzed subsequently by the azomethine H method (Lohse 1982) by the Soil and Plant Testing Laboratory at the University of Missouri.

The *bx3* mutants in the B73 background and the B73 inbreds (control) or *bx3* segregating lines were grown in the summers of 2020, 2021, and 2023 at the field station of the University of Bonn (Bonn-Endenich, Germany), where soil boron concentration was 0.27 mg/kg as assessed using a cold 0.01 M $CaCl_2$ extraction protocol and a miniaturized curcumin method for analysis (Wimmer and Goldbach 1999). Four ear leaves of *bx3* mutants, the B73 inbreds or the wild-type sibling controls were pooled separately, 2 cm of the leaf tips were discarded and the remaining leaf blades dried at 60 °C, and ground to a fine powder (3 biological replicates). For the Arabidopsis samples, whole rosettes were taken before bolting and dried at 60 °C before grinding to a fine powder

(3 to 4 biological replicates). Plant samples (500 mg maize or Arabidopsis) were digested with nitric acid in a CEM Mars 5 microwave digestion system (CEM Corporation, Matthews, North Carolina, USA) and boron concentration was analyzed by a miniaturized curcumin method (Wimmer and Goldbach 1999).

Genome-wide association study

The outlier removal, optimal transformation and BLUP calculation for the trait were performed as described in Slaten et al. (2020). The genotypic dataset was previously described in Shrestha et al. (2022). Briefly, the association panel was previously genotyped with the Illumina MaizeSNP50 BeadChip (Cook et al. 2012) and also with a genotyping-by-sequencing approach (Elshire et al. 2011) as described and utilized in Lipka et al. (2013). SNPs were filtered using minor allele frequency >0.05 and a total of 458,775 SNPs from both datasets were used for the GWAS analysis. We used FarmCPU model (Liu et al. 2016) to conduct GWAS and Bonferroni correction was used to correct for multiple testing at 5%. The candidate gene list was obtained using a 200 kb window size (100 kb on either side) of the significant SNPs. This interval was chosen to cover the long range LD in maize and also to compensate for low marker coverage as described in Ching et al. (2002), Flint-Garcia et al. (2003), Yan et al. (2009), and Shrestha et al. (2022). The physical locations and annotations of the genes were based on v2 of the maize B73 annotation.

Correlation analysis between boron concentrations and GWAS candidate gene expression in the Goodman-Buckler association panel

For the correlation analysis between leaf boron concentration and target gene expression levels, Pearson correlation tests were performed. We used gene expression data from Kremling et al. (2018). The authors collected 3′ RNA-sequencing data from 7 different tissues from 255 inbred lines of the Goodman-Buckler association panel. The normalized gene expression levels of candidate genes were used and correlated with back-transformed BLUPs of leaf boron concentrations of 277 lines of the Goodman-Buckler association panel (Supplementary Table S1).

Phenotypic analyses

Plant height measurements were taken at maturity from the soil level up to the tip of the tassel (total plant height = PH) and to the leaf collar of the flag leaf (plant height to flag leaf = FL). In addition, the number of primary tillers was scored. Plant height at seedling stage was determined from the pot soil level to the top of the leaf whorl. Developmental stages were assessed by using V-stages (Abendroth et al. 2011) and leaf number is given as the number of fully developed leaves plus all leaves that have emerged from the whorl.

TL was determined by measuring the length from the tassel node (node where the tassel is inserted in the stem at the base of the flag leaf) to the tip of the tassel. Peduncle length (PL) was determined by measuring the length of the tassel from the tassel node to the first branch. Branching area (BA) was determined by measuring the length of the main spike between the first and the last branch. Branch number (BN) is the total number of primary tassel branches. The length of CS was determined by subtracting PL and BA from TL.

Boron toxicity symptoms in seedling leaves were assessed using an adapted leaf bronzing score (de Abreu Neto et al. 2017), where 0 = no phenotype, 1 = leaf tips senesced, 2 = leaf tip and edges senesced (with or without leaf rolling), 3 = senescence reaches into leaf blade (with or without leaf rolling), 4 = any or all symptoms of categories 1 to 3 including aberrant leaf morphology, and 5 = fully senesced leaf (Supplementary Fig. S4).

The percentage of the senesced leaf area (boron fertilization experiment) was assessed 14 DAP (developmental stage V2 with 3 to 4 emerged leaves). The entire leaf blade of leaf one was cut and photographed, while for leaf 2, 5 cm of the leaf tip were cut and photographed. Image analysis was done with ImageJ (Schneider et al. 2012). The thresholds of all images were adjusted to either provide the full leaf area or the area of senescence (Supplementary Fig. S8). Out of these 2 values, the percentage of the senesced leaf area for every leaf was calculated.

Boron fertilization

B73 and *bx3* seedlings in the B73 background were grown in ED73 soil in a walk-in growth chamber (26 °C day, 16 °C night, 16 h day, 8 h light, 70% humidity) for 14 d and watered with either ultra-pure water (Merck Millipore, Burlington, USA), Peter's fertilizer (ICL specialty fertilizers, Tel-Aviv, Israel), Peter's fertilizer +0.5 mM boric acid, or Peter's fertilizer +1 mM boric acid. For the regular strength of Peter's fertilizer, nitrogen levels were adjusted to 238 ppm, which resulted in a final boron concentration of 0.08 ppm (Matthes et al. 2018). The plants were watered every other day, where 1 L of the respective solution was given to 24 plants (12 plants per genotype). The experiment was repeated 3 times.

DIMBOA levels in the *tls1* mutant

The boron transporter mutant *Zmtls1* (Durbak et al. 2014; Leonard et al. 2014) and wild-type siblings were grown in the Sears greenhouse facility at the University of Missouri, Columbia, USA (16/8 h light/dark cycle with an average day temperature of 30.5 °C, an average night temperature of 25 °C, and average humidity of 40% (day) and 60% (night)) and were continuously fertilized with Peter's fertilizer (ICL specialty fertilizers, Tel-Aviv, Israel), where nitrogen levels were adjusted to 238 ppm, resulting in boron concentrations of 0.08 ppm (Matthes et al. 2018). Developing leaves were dissected as described in Matthes et al. (2022) and analyzed for DIMBOA concentrations using liquid chromatography-mass spectrometry by the proteomics and metabolomics core facility at the University of Nebraska—Lincoln, USA. For details, see Supplementary Methods.

Boron-(H)ION complex formation

A solution of boric acid (2.6 mg/mL in D2O, pH 6, 540 μL, 22.5 μmol, 1.0 eq.) was added to a solution of ION (Sigma-Aldrich) (50 mg/mL in DMSO, 60 μL, 22.5 μmoL, 1.0 eq.) and kept at room temperature for 80 h. ^{11}B-NMR spectra were recorded after mixing, 18 and 80 h. Further experiments were performed with a boric acid solution, adjusted to pH 8 using 0.5 M NaOH solution, either at room temperature or 80 °C. Spectra were recorded on a Bruker Avance Neo 400 MHz with CryoProbe. Chemical shifts are given in ppm.

A solution of boric acid (2.3 mg/mL in D2O, pH 8 (adjusted using 0.5 M NaOH solution), 540 μL, 20.1 μmol, 1.0 eq.) was added to a solution of HION (Sigma-Aldrich) (50 mg/mL in DMSO, 60 μL, 20.1 μmol, 1.0 eq.) and kept either at room temperature or 80 °C. ^{11}B-NMR spectra were recorded after mixing, 3, 18, and 40 h. Further experiments were performed with 10 eq. HION (500 mg/mL in DMSO, 60 μL, 201 μmol, 10 eq.), 0.5 eq. and 0.2 eq. HION (respective stock solutions). The oxidized product isatin was isolated using preparative thin layer chromatography (CH/AcOEt 1:1).

Control experiments were performed in the absence of boric acid and using dimethylformamide instead of DMSO, also giving isatin as a product.

Under an argon atmosphere, tetrabutylammonium hydroxide (90.0 µL, 184 µmoL, 55 w% solution in water, 0.55 eq) was added to a degassed solution of HION (Sigma-Aldrich) (50.0 mg, 335 µmol, 1.00 eq) and boric acid (11.4 mg, 184 µmol, 0.55 eq.) in dimethylformamide (15 mL). The resulting solution was stirred at 130 °C for 16 h. Subsequently, the solvent was removed under reduced pressure using a cooling trap (<0.001 mbar, 100 °C). The yellow-brown color of the crude product mixture changes immediately to a strong violet color upon contact with air. The ^{11}B-NMR and ^{1}H-NMR spectra of the yellow-brown mixture were measured in a quartz glass NMR tube under argon atmosphere, using anhydrous and degassed acetonitrile-d_3 as a solvent.

To verify the origin of additional species in these spectra, the control experiments were performed (i) between the base and boric acid in the absence of HION and (ii) between HION and the base in the absence of boric acid, and the crude products were analyzed by ^{1}H and ^{11}B-NMR spectroscopy.

The spectra were recorded on a Bruker Avance 400 NMR spectrometer. Chemical shifts are given in ppm.

Statistical analysis

Statistical significance of the boron concentrations in the *bx3* mutant, the various growth trait phenotypes between *bx3* and B73 siblings, and the DIMBOA levels in the *tls1* mutant in comparison to non-mutant control lines was assessed in Microsoft Excel using Student's *t*-test (Student 1908) at a significance level of $P < 0.05$.

Statistical significance at a significance level of $P < 0.05$ was determined for the different boron fertilization treatments and the different genotypic categories in the Arabidopsis lines using analysis of variance with post hoc multiple testing correction applying the Tukey or Benjamini-Hochberg algorithms using the multcompView (Piepho 2004), agricolae (de Menidburu and Yaseen 2020), and emmeans (Lenth 2022) packages in R.

Accession numbers

Sequence data from this article can be found in the GenBank/EMBL data libraries or the MaizeGDB database under the following accession numbers: *Zmbx3*, LOC103652724, Zm00001eb165550; *Zmbx1*, LOC542117, Zm00001eb165610; *Zmbx2*, LOC100192631, Zm00001eb165620; *Zmtls1*, LOC541885, Zm00001eb043650.

Acknowledgments

Author contributions

V.S.: BLUPs and back-transformed BLUPs generation, GWAS analysis, correlation analysis, data analysis. L.C: Boron concentration measurements in soil, *bx3* mutants and Arabidopsis lines, data analysis, phenotypic analysis. C.S.: Phenotypic analysis of Arabidopsis lines and *bx3* mutants. J.N., T.D.: Boron–benzoxazinoid complex experiments. G. M., Z. D., T. K.: Boron analysis 282 Goodman-Buckler association panel. A.A: Generation and propagation of the Arabidopsis lines used. M.F., A.N.K., H.J., G.S., F.H., P.M., R.A.: Experimental design, student supervision, and data analysis. M.M.: Conceived and designed the study, experimental design, data analysis, student supervision, and writing of the manuscript with input from all authors. All authors approved of the final version of this manuscript.

Supplementary data

The following materials are available in the online version of this article.

Supplementary Materials and Methods.

Supplementary Figure S1. Phenotype of the *Zmtls1* mutant grown in the field in Bonn-Endenich or in the greenhouse and boron concentrations of *bx3* mutants.

Supplementary Figure S2. Phenotypes induced by boron supplementation and boron concentration in WT and *bx3* ear leaves grown in the greenhouse.

Supplementary Figure S3. Leaf necrosis and tassel phenotypes of the *bx3* mutant grown in the field Bonn-Endenich (2020).

Supplementary Figure S4. Scoring scheme for assessing leaf necrosis.

Supplementary Figure S5. Benzoxazinoid biosynthesis pathway in maize and lactam/lactim tautomerism of HION.

Supplementary Figure S6. Reactions of indolin-2-one (ION) and 3-hydroxy-ION in presence of air.

Supplementary Figure S7. Boric acid reacts with HION to form additional boron species. **A)** The ^{1}H-NMR spectra showing the crude mixture of the reaction of HION with boric acid in the presence of a base, **B)** the control experiment without boric acid, and **C)** pure HION.

Supplementary Figure S8. Image segmentation using ImageJ (Schneider et al. 2012).

Supplementary Table S1. Boron concentration of maize ear leaves in 277 lines of the 282 Goodman-Buckler association.

Supplementary Table S2. Descriptive statistics summary of boron concentrations (µg/g dw) obtained from the 277 back-transformed BLUPs of the 282 Goodman-Buckler association panel. dw, dry weight.

Supplementary Table S3. Correlation between gene expression of candidate genes with boron concentration in 277 lines of the 282 Goodman-Buckler association panel.

Supplementary Table S4. IPC-OES analysis of various nutrients in B73 and *bx3* mutants.

Supplementary Table S5. Phenotypes at maturity of *bx1*, *bx2*, *bx3* mutants, and their respective inbred line controls (B73, W22).

Supplementary Table S6. Vegetative phenotypes of *bx3* mutants and B73 control plants 14 and 25 days after planting (DAP).

Supplementary Table S7. Vegetative phenotypes of *bx3* mutants and B73 control plants 14 days after planting (DAP) with different watering regimes.

Supplementary Table S8. Correlation analysis of *bx* gene expression with boron concentration in the 282 Goodman-Buckler association panel.

Funding

Conflict of interest statement. None declared.

Data availability

All data are incorporated into the article and its online supplementary material.

References

Abendroth LJ, Elmore RW, Boyer MJ, Marlay SK (2011) Corn growth and development. Ext. Publ. #PMR-1009. https://store.extension.iastate.edu/Product/Corn-Growth-and-Development.

Abramov A, Hoffmann T, Stark TD, Zheng L, Lenk S, Hammerl R, Lanzl T, Dawid C, Schön CC, Schwab W, *et al.* Engineering of benzoxazinoid biosynthesis in *Arabidopsis thaliana*: metabolic and physiological challenges. *Phytochemistry*. 2021:192:112947. https://doi.org/10.1016/j.phytochem.2021.112947

Abreu I, Poza L, Bonilla I, Bolaños L. Boron deficiency results in early repression of a cytokinin receptor gene and abnormal cell differentiation in the apical root meristem of *Arabidopsis thaliana*. *Plant Physiol Biochem*. 2014:77:117–121. https://doi.org/10.1016/j.plaphy.2014.02.008

Ahmad S, Veyrat N, Gordon-Weeks R, Zhang Y, Martin J, Smart L, Glauser G, Erb M, Flors V, Frey M, *et al.* Benzoxazinoid metabolites regulate innate immunity against aphids and fungi in maize. *Plant Physiol*. 2011:157(1):317–327. https://doi.org/10.1104/pp.111.180224

Alva O, Roa-Roco RN, Pérez-Díaz R, Yánez M, Tapia J, Moreno Y, Ruiz-Lara S, González E, Gerós H. Pollen morphology and boron concentration in floral tissues as factors triggering natural and GA-induced parthenocarpic fruit development in grapevine. *PLoS One*. 2015:10(10):e0139503. https://doi.org/10.1371/journal.pone.0139503

Aquea F, Federici F, Moscoso C, Vega A, Jullian P, Haseloff J, Arce-Johnson P. A molecular framework for the inhibition of Arabidopsis root growth in response to boron toxicity. *Plant Cell Environ*. 2012:35(4):719–734. https://doi.org/10.1111/j.1365-3040.2011.02446.x

Begum RA, Fry SC. Boron bridging of rhamnogalacturonan-II in Rosa and Arabidopsis cell cultures occurs mainly in the endomembrane system and continues at a reduced rate after secretion. *Ann Bot*. 2022:130(5):703–715. https://doi.org/10.1093/aob/mcac119

Brdar-Jokanović M. Boron toxicity and deficiency in agricultural plants. *Int J Mol Sci*. 2020:21(4):1424. https://doi.org/10.3390/ijms21041424

Brown PH, Shelp BJ. Boron mobility in plants. *Plant Soil*. 1997:193(2):85–101. https://doi.org/10.1023/A:1004211925160

Camacho-Cristóbal JJ, Martín-Rejano EM, Herrera-Rodríguez MB, Navarro-Gochicoa MT, Rexach J, González-Fontes A. Boron deficiency inhibits root cell elongation via an ethylene/auxin/ROS-dependent pathway in Arabidopsis seedlings. *J Exp Bot*. 2015:66(13):3831–3840. https://doi.org/10.1093/jxb/erv186

Chatterjee M, Liu Q, Menello C, Galli M, Gallavotti A. The combined action of duplicated boron transporters is required for maize growth in boron-deficient conditions. *Genetics*. 2017:206(4):2041–2051. https://doi.org/10.1534/genetics.116.198275

Chatterjee M, Tabi Z, Galli M, Malcomber S, Buck A, Muszynski M, Gallavotti A. The boron efflux transporter ROTTEN EAR is required for maize inflorescence development and fertility. *Plant Cell*. 2014:26(7):2962–2977. https://doi.org/10.1105/tpc.114.125963

Ching A, Caldwell KS, Jung M, Dolan M, Oscar S, Smith H, Tingey S, Morgante M, Rafalski AJ. SNP frequency, haplotype structure and linkage disequilibrium in elite maize inbred lines. *BMC Genet*. 2002:14:1–14. https://doi.org/10.1186/1471-2156-3-19

Choi EY, Kolesik P, McNeill A, Collins H, Zhang Q, Huynh BL, Graham R, Stangoulis J. The mechanism of boron tolerance for maintenance of root growth in barley (*Hordeum vulgare* L.). *Plant Cell Environ*. 2007:30(8):984–993. https://doi.org/10.1111/j.1365-3040.2007.01693.x

Chormova D, Fry SC. Boron bridging of rhamnogalacturonan-II is promoted *in vitro* by cationic chaperones, including polyhistidine and wall glycoproteins. *New Phytol*. 2016:209(1):241–251. https://doi.org/10.1111/nph.13596

Chormova D, Messenger DJ, Fry SC. Boron bridging of rhamnogalacturonan-II, monitored by gel electrophoresis, occurs during polysaccharide synthesis and secretion but not postsecretion. *Plant J*. 2014:77(4):534–546. https://doi.org/10.1111/tpj.12403

Cook JP, McMullen MD, Holland JB, Tian F, Bradbury P, Ross-Ibarra J, Buckler ES, Flint-Garcia SA. Genetic architecture of maize kernel composition in the nested association mapping and inbred association panels. *Plant Physiol*. 2012:158(2):824–834. https://doi.org/10.1104/pp.111.185033

de Abreu Neto BJ, Hurtado-perez MC, Wimmer MA, Frei M. Genetic factors underlying boron toxicity tolerance in rice: genome-wide association study and transcriptomic analysis. *J Exp Bot*. 2017:68(3):687–700. https://doi.org/10.1093/jxb/erw423

de Bruijn WJC, Gruppen H, Vincken JP. Structure and biosynthesis of benzoxazinoids: plant defence metabolites with potential as antimicrobial scaffolds. *Phytochemistry*. 2018:155:233–243. https://doi.org/10.1016/j.phytochem.2018.07.005

de Menidburu F, Yaseen M. agricolae: statistical procedures for agricultural research. R package version 1.4.0. 2020. https://github.com/myaseen208/agricolae.

Durbak AR, Phillips KA, Pike S, O'Neill MA, Mares J, Gallavotti A, Malcomber ST, Gassmann W, McSteen P. Transport of boron by the *tassel-less1* aquaporin is critical for vegetative and reproductive development in maize. *Plant Cell*. 2014:26(7):2978–2995. https://doi.org/10.1105/tpc.114.125898

Eaton FM. Deficiency, toxicity, and accumulation of boron in plants. *J Agric Res*. 1944:69:237–277.

Eggert K, von Wirén N. Response of the plant hormone network to boron deficiency. *New Phytol*. 2017:216(3):868–881. https://doi.org/10.1111/nph.14731

Elshire RJ, Glaubitz JC, Sun Q, Poland JA, Kawamoto K, Buckler ES, Mitchell SE. A robust, simple genotyping-by-sequencing (GBS) approach for high diversity species. *PLoS One*. 2011:6(5):e19379. https://doi.org/10.1371/journal.pone.0019379

Esim N, Tiryaki D, Karadagoglu O, Atici O. Toxic effects of boron on growth and antioxidant system parameters of maize (*Zea mays* L.) roots. *Toxicol Ind Health*. 2013:29(9):800–805. https://doi.org/10.1177/0748233712442729

Feng Y, Cui R, Wang S, He M, Hua Y, Shi L, Ye X, Xu F. Transcription factor BnaA9.WRKY47 contributes to the adaptation of *Brassica napus* to low boron stress by up-regulating the boric acid channel gene *BnaA3.NIP5;1*. *Plant Biotechnol J*. 2020:18(5):1241–1254. https://doi.org/10.1111/pbi.13288

Flint-Garcia SA, Thornsberry JM, Buckler ESI. Structure of linkage disequilibrium in plants. *Annu Rev Plant Biol*. 2003:54(1):357–374. https://doi.org/10.1146/annurev.arplant.54.031902.134907

Flint-Garcia SA, Thuillet AC, Yu J, Pressoir G, Romero SM, Mitchell SE, Doebley J, Kresovich S, Goodman MM, Buckler ES. Maize association population: a high-resolution platform for quantitative trait locus dissection. *Plant J*. 2005:44(6):1054–1064. https://doi.org/10.1111/j.1365-313X.2005.02591.x

Florean M, Luck K, Hong B, Nakamura Y, O'Connor SE, Köllner TG. Reinventing metabolic pathways: independent evolution of benzoxazinoids in flowering plants. *Proc Natl Acad Sci U S A*. 2023:120(42):e2307981120. https://doi.org/10.1073/pnas.2307981120

Frey M, Chomet P, Glawischnig E, Stettner C, Grün S, Winklmair A, Eisenreich W, Bacher A, Meeley RB, Briggs SP, *et al.* Analysis of a chemical plant defense mechanism in grasses. *Science*. 1997:277(5326):696–699. https://doi.org/10.1126/science.277.5326.696

Frey M, Kliem R, Saedler H, Gierl A. Expression of a cytochrome P450 gene family in maize. *Mol Genet Genomics*. 1995:246(1):100–109. https://doi.org/10.1007/BF00290138

Frey M, Schullehner K, Dick R, Fiesselmann A, Gierl A. Benzoxazinoid biosynthesis, a model for evolution of secondary metabolic pathways in plants. *Phytochemistry*. 2009:70(15–16):1645–1651. https://doi.org/10.1016/j.phytochem.2009.05.012

Gómez-Soto D, Galván S, Rosales E, Bienert P, Abreu I, Bonilla I, Bolaños L, Reguera M. Insights into the role of phytohormones regulating *pAtNIP5;1* activity and boron transport in *Arabidopsis thaliana*. *Plant Sci*. 2019:287:110198. https://doi.org/10.1016/j.plantsci.2019.110198

Hamilton R. A corn mutant deficient in 2,4-dihydroxy-7-methoxy-1,4-benzoxazin-3-one with an altered tolerance of atrazine. *Weeds*. 1964:12(1):27–30. https://doi.org/10.2307/4040633

Hassan M, Oldach K, Baumann U, Langridge P, Sutton T. Genes mapping to boron tolerance QTL in barley identified by suppression subtractive hybridization. *Plant Cell Environ*. 2010:33(2):188–198. https://doi.org/10.1111/j.1365-3040.2009.02069.x

Hayes JE, Pallotta M, Garcia M, Öz MT, Rongala J, Sutton T. Diversity in boron toxicity tolerance of Australian barley (*Hordeum vulgare* L.) genotypes. *BMC Plant Biol*. 2015:15(1):231. https://doi.org/10.1186/s12870-015-0607-1

He M, Wang S, Zhang C, Liu L, Zhang J, Qiu S, Wang H, Yang G, Xue S, Shi L, *et al.* Genetic variation of *BnaA3.NIP5;1* expressing in the lateral root cap contributes to boron deficiency tolerance in *Brassica napus*. *PLoS Genet*. 2021:17(7):e1009661. https://doi.org/10.1371/journal.pgen.1009661

Heckmann JR. Boron: needs of soils and crops in New Jersey. Rutgers NJAES Cooperative Extension; 2009.

Hiroguchi A, Sakamoto S, Mitsuda N, Miwa K. Golgi-localized membrane protein AtTMN1/EMP12 functions in the deposition of rhamnogalacturonan II and I for cell growth in Arabidopsis. *J Exp Bot*. 2021:72(10):3611–3629. https://doi.org/10.1093/jxb/erab065

Housh AB, Matthes MS, Gerheart A, Wilder SL, Kil K, Schueller M, GuthrieJM, Mcsteen P, Ferrieri R. Assessment of a ^{18}F-phenylboronic acid radiotracer for imaging boron in maize. *Int J Mol Sci*. 2020:21(3):976. https://doi.org/10.3390/ijms21030976

Hu L, Mateo P, Ye M, Zhang X, Berset JD, Handrick V, Radisch D, Grabe V, Köllner TG, Gershenzon J, *et al.* Plant iron acquisition strategy exploited by an insect herbivore. *Science*. 2018:361(6403):694–697. https://doi.org/10.1126/science.aat4082

Huai Z, Peng L, Wang S, Zhao H, Shi L, Xu F. Identification and characterization of an *Arabidopsis thaliana* mutant *lbt* with high tolerance to boron deficiency. *Front Plant Sci*. 2018:9:736. https://doi.org/10.3389/fpls.2018.00736

Jefferies SP, Barr AR, Karakousis A, Kretschmer JM, Manning S, Chalmers KJ, Nelson JC, Islam AKMR, Langridge P. Mapping of chromosome regions conferring boron toxicity tolerance in barley (*Hordeum vulgare* L.). *Theor Appl Genet*. 1999:98(8):1293–1303. https://doi.org/10.1007/s001220051195

Jefferies SP, Pallotta MA, Paull JG, Karakousis A, Kretschmer JM, Manning S, Islam AKMR, Langridge P, Chalmers KJ. Mapping and validation of chromosome regions conferring boron toxicity tolerance in wheat (*Triticum aestivum*). *Theor Appl Genet*. 2000:101(5–6):767–777. https://doi.org/10.1007/s001220051542

Jia Z, Bienert MD, von Wirén N, Bienert GP. Genome-wide association mapping identifies *HvNIP2;2/HvLsi6* accounting for efficient boron transport in barley. *Physiol Plant*. 2021:171(4):809–822. https://doi.org/10.1111/ppl.13340

Kasajima I, Fujiwara T. Identification of novel *Arabidopsis thaliana* genes which are induced by high levels of boron. *Plant Biotechnol*. 2007:24(3):355–360. https://doi.org/10.5511/plantbiotechnology.24.355

Kasajima I, Ide Y, Yokota Hirai M, Fujiwara T. WRKY6 is involved in the response to boron deficiency in *Arabidopsis thaliana*. *Physiol Plant*. 2010:139(1):80–92. https://doi.org/10.1111/j.1399-3054.2010.01349.x

Kato Y, Miwa K, Takano J, Wada M, Fujiwara T. Highly boron deficiency-tolerant plants generated by enhanced expression of NIP5;1, a boric acid channel. *Plant Cell Physiol*. 2009:50(1):58–66. https://doi.org/10.1093/pcp/pcn168

Kobayashi M, Matoh T, Azuma J. Two chains of rhamnogalacturonan II are cross-linked by borate-diol ester bonds in higher plant cell walls. *Plant Physiol*. 1996:110(3):1017–1020. https://doi.org/10.1104/pp.110.3.1017

Kremling KAG, Chen SY, Su MH, Lepak NK, Romay MC, Swarts KL, Lu F, Lorant A, Bradbury PJ, Buckler ES. Dysregulation of expression correlates with rare-allele burden and fitness loss in maize. *Nature*. 2018:555(7697):520–523. https://doi.org/10.1038/nature25966

Landi M, Margaritopoulou T, Papadakis IE, Araniti F. Boron toxicity in higher plants: an update. *Planta*. 2019:250(4):1011–1032. https://doi.org/10.1007/s00425-019-03220-4

Lenth RV. emmeans: estimated marginal means, aka least-squares means. R package version 1.7.2. 2022. https://CRAN.Rproject.org/package=emmeans.

Leonard A, Holloway B, Guo M, Rupe M, Yu G, Beatty M, Zastrow-Hayes G, Meeley R, Llaca V, Butler K, *et al.* Tassel-less1 encodes a boron channel protein required for inflorescence development in maize. *Plant Cell Physiol*. 2014:55(6):1044–1054. https://doi.org/10.1093/pcp/pcu036

Li K, Kamiya T, Fujiwara T. Differential roles of PIN1 and PIN2 in root meristem maintenance under low-B conditions in *Arabidopsis thaliana*. *Plant Cell Physiol*. 2015:56(6):1205–1214. https://doi.org/10.1093/pcp/pcv047

Lipka AE, Gore MA, Magallanes-Lundback M, Mesberg A, Lin H, Tiede T, Chen C, Robin Buell C, Buckler ES, Rocheford T, *et al.* Genome-wide association study and pathway-level analysis of tocochromanol levels in maize grain. *G3 (Bethesda, Md.)*. 2013:3(8):1287–1299. https://doi.org/10.1534/g3.113.006148

Liu X, Huang M, Fan B, Buckler ES, Zhang Z. Iterative usage of fixed and random effect models for powerful and efficient genome-wide association studies. *PLoS Genet*. 2016:12(2):e1005767. https://doi.org/10.1371/journal.pgen.1005767

Lohse G. Microanalytical azomethine-H method for boron determination in plant tissue. *Commun Soil Sci Plant Anal*. 1982:13(2): 127–134. https://doi.org/10.1080/00103628209367251

Lordkaew S, Dell B, Jamjod S, Rerkasem B. Boron deficiency in maize. *Plant Soil*. 2011:342(1–2):207–220. https://doi.org/10.1007/s11104-010-0685-7

Lv Q, Wang L, Wang JZ, Li P, Chen YL, Du J, He YK, Bao F. SHB1/HY1 alleviates excess boron stress by increasing BOR4 expression level and maintaining boron homeostasis in Arabidopsis roots. *Front Plant Sci*. 2017:8:790. https://doi.org/10.3389/fpls.2017.00790

Marschner P. ed. *Marschner's mineral nutrition of higher plants*. 3rd ed. Amsterdam: Elsevier Ltd; 2012.

Martín-Rejano EM, Camacho-Cristóbal JJ, Herrera-Rodríguez MB, Rexach J, Navarro-Gochicoa MT, González-Fontes A. Auxin and ethylene are involved in the responses of root system architecture to low boron supply in Arabidopsis seedlings. *Physiol Plant*. 2011:142(2): 170–178. https://doi.org/10.1111/j.1399-3054.2011.01459.x

Matoh T, Kawaguchi S, Kobayashi M. Ubiquity of a borate-rhamnogalacturonan II complex in the cell walls of higher plants. *Plant Cell Physiol*. 1996:37(5):636–640. https://doi.org/10.1093/oxfordjournals.pcp.a028992

Matthes M, Torres-Ruiz RA. Boronic acid treatment phenocopies *monopteros* by affecting PIN1 membrane stability and polar auxin transport in *Arabidopsis thaliana* embryos. *Development*. 2016: 143(21):4053–4062. https://doi.org/10.1242/dev.131375

Matthes MS, Best NB, Robil JM, McSteen P. Enhancement of developmental defects in the boron-deficient maize mutant *tassel-less1* by reduced auxin levels. *J Plant Nutr Soil Sci*. 2023. https://doi.org/10.1002/jpln.202300155

Matthes MS, Darnell Z, Best NB, Guthrie K, Robil JM, Amstutz J, Durbak A, McSteen P. Defects in meristem maintenance, cell division, and cytokinin signaling are early responses in the boron deficient maize mutant *tassel-less1*. *Physiol Plant*. 2022:174(2): e13670. https://doi.org/10.1111/ppl.13670

Matthes MS, Robil JM, McSteen P. From element to development: the power of the essential micronutrient boron to shape morphological processes in plants. *J Exp Bot*. 2020:71(5):1681–1693. https://doi.org/10.1093/jxb/eraa042

Matthes MS, Robil JM, Tran T, Kimble A, Mcsteen P. Increased transpiration is correlated with reduced boron deficiency symptoms in the maize *tassel-less1* mutant. *Physiol Plant*. 2018:163(3): 344–355. https://doi.org/10.1111/ppl.12717

Miwa K, Takano J, Fujiwara T. Improvement of seed yields under boron-limiting conditions through overexpression of BOR1, a boron transporter for xylem loading, in *Arabidopsis thaliana*. *Plant J*. 2006:46(6): 1084–1091. https://doi.org/10.1111/j.1365-313X.2006.02763.x

Noguchi K, Yasumori M, Imai T, Naito S, Matsunaga T, Oda H. *bor1-1*, an *Arabidopsis thaliana* mutant that requires a high level of boron. *Plant Physiol*. 1997:115(3):901–906. https://doi.org/10.1104/pp.115.3.901

O'Neill MA, Eberhard S, Albersheim P, Darvill AG. Requirement of borate cross-linking of cell wall rhamnogalacturonan-II for Arabidopsis growth. *Science*. 2001:294(5543):846–849. https://doi.org/10.1126/science.1062319

O'Neill MA, Warrenfeltz D, Kates K, Pellerin P, Doco T, Darvill AG, Albersheim P. Rhamnogalacturonan-II, a pectic polysaccharide in the walls of growing plant cell, forms a dimer that is covalently cross-linked by a borate ester. In vitro conditions for the formation and hydrolysis of the dimer. *J Biol Chem*. 1996:271(37): 22923–22930. https://doi.org/10.1074/jbc.271.37.22923

Onuh AF, Miwa K. Regulation, diversity and evolution of boron transporters in plants. *Plant Cell Physiol*. 2021:62(4):590–599. https://doi.org/10.1093/pcp/pcab025

Onuh AF, Miwa K. Mutations in type II Golgi-localized proton pyrophosphatase AVP2;1/VHP2;1 affect pectic polysaccharide rhamnogalacturonan-II and alter root growth under low boron condition in *Arabidopsis thaliana*. *Front Plant Sci*. 2023:14:1255486. https://doi.org/10.3389/fpls.2023.1255486

Pallotta M, Schnurbusch T, Hayes J, Hay A, Baumann U, Paull J, Langridge P, Sutton T. Molecular basis of adaptation to high soil boron in wheat landraces and elite cultivars. *Nature*. 2014: 514(7520):88–91. https://doi.org/10.1038/nature13538

Paull JG, Rathjen AJ, Cartwright B. Major gene control of tolerance of bread wheat (*Triticum aestivum* L.) to high concentrations of soil boron. *Euphytica*. 1991:55(3):217–228. https://doi.org/10.1007/BF00021242

Peng L, Shi L, Cai H, Xu F, Zeng C. Transcriptional profiling reveals adaptive responses to boron deficiency stress in Arabidopsis. *Z Naturforsch—Sect C J Biosci*. 2012:67:510–524. https://doi.org/10.1515/znc-2012-9-1009

Piepho HP. An algorithm for a letter-based representation of all-pairwise comparisons. *J Comput Graph Stat*. 2004:13(2):456–466. https://doi.org/10.1198/1061860043515

Pommerrenig B, Faber M, Hajirezaei M-R, von Wirén N, Bienert GP. Cytokinins as boron deficiency signals to sustain shoot development in boron-efficient oilseed rape. *Physiol Plant*. 2022:174(5): e13776. https://doi.org/10.1111/ppl.13776

Pommerrenig B, Junker A, Abreu I, Bieber A, Fuge J, Willner E, Bienert MD, Altmann T, Bienert GP. Identification of rapeseed (*Brassica napus*) cultivars with a high tolerance to boron-deficient conditions. *Front Plant Sci*. 2018:9:1142. https://doi.org/10.3389/fpls.2018.01142

Poza-Viejo L, Abreu I, González-García MP, Allauca P, Bonilla I, Bolanos L, Reguera M. Boron deficiency inhibits root growth by controlling meristem activity under cytokinin regulation. *Plant Sci*. 2018:270: 176–189. https://doi.org/10.1016/j.plantsci.2018.02.005

Reid RJ, Hayes JE, Post A, Stangoulis JCR, Graham RD. A critical analysis of the causes of boron toxicity in plants. *Plant Cell Environ*. 2004:27(11):1405–1414. https://doi.org/10.1111/j.1365-3040.2004.01243.x

Sakamoto T, Inui YT, Uraguchi S, Yoshizumi T, Matsunaga S, Mastui M, Umeda M, Fukui K, Fujiwara T. Condensin II alleviates DNA damage and is essential for tolerance of boron overload stress in Arabidopsis. *Plant Cell*. 2011:23(9):3533–3546. https://doi.org/10.1105/tpc.111.086314

Schaefer RJ, Michno JM, Jeffers J, Hoekenga O, Dilkes B, Baxter I, Myersc CL. Integrating coexpression networks with GWAS to prioritize causal genes in maize. *Plant Cell*. 2018:30(12):2922–2942. https://doi.org/10.1105/tpc.18.00299

Schneider CA, Rasband WS, Eliceiri KW. NIH image to ImageJ: 25 years of image analysis. *Nat Methods*. 2012:9(7):671–675. https://doi.org/10.1038/nmeth.2089

Schnurbusch T, Hayes J, Hrmova M, Baumann U, Ramesh SA, Tyerman SD, Langridge P, Sutton T. Boron toxicity tolerance in barley through reduced expression of the multifunctional aquaporin *HvNIP2;1*. *Plant Physiol*. 2010:153(4):1706–1715. https://doi.org/10.1104/pp.110.158832

Sechet J, Htwe S, Urbanowicz B, Agyeman A, Feng W, Ishikawa T, Colomes M, Kumar KS, Kawai-yamada M, Dinneny JR, *et al.* Suppression of Arabidopsis GGLT1 affects growth by reducing the L-galactose content and borate cross-linking of rhamnogalacturonan-II. *Plant J*. 2018:96(5):1036–1050. https://doi.org/10.1111/tpj.14088

Shrestha V, Yobi A, Slaten ML, Chan YO, Holden S, Gyawali A, Flint-Garcia S, Lipka AE, Angelovici R. Multiomics approach reveals a role of translational machinery in shaping maize kernel amino acid composition. *Plant Physiol*. 2022:188(1):111–133. https://doi.org/10.1093/plphys/kiab390

Slaten ML, Chan YO, Shrestha V, Lipka AE, Angelovici R. HAPPI GWAS: holistic analysis with pre- and post-integration GWAS. *Bioinformatics*. 2020:36(17):4655–4657. https://doi.org/10.1093/bioinformatics/btaa589

Sommer AL, Sorokin H. Effects of the absence of boron and of some other essential elements on the cell and tissue structure of the root tips of *Pisum sativum*. *Plant Physiol*. 1928:3(3):237–260.1. https://doi.org/10.1104/pp.3.3.237

Student. The probable error of a mean. *Biometrika*. 1908:6(1):1–25. https://doi.org/10.2307/2331554

Sutton T, Baumann U, Hayes J, Collins NC, Shi BJ, Schnurbusch T, Hay A, Mayo G, Pallotta M, Tester M, *et al*. Boron-toxicity tolerance in barley arising from efflux transporter amplification. *Science*. 2007:318(5855):1446–1449. https://doi.org/10.1126/science.1146853

Takano J, Wada M, Ludewig U, Schaaf G, von Wiren N, Fujiwara T. The Arabidopsis major intrinsic protein NIP5;1 is essential for efficient boron uptake and plant development under boron limitation. *Plant Cell*. 2006:18(6):1498–1509. https://doi.org/10.1105/tpc.106.041640

Tzin V, Fernandez-Pozo N, Richter A, Schmelz EA, Schoettner M, Schäfer M, Ahern KR, Meihls LN, Kaur H, Huffaker A, *et al*. Dynamic maize responses to aphid feeding are revealed by a time series of transcriptomic and metabolomic assays. *Plant Physiol*. 2015:169(3):1727–1743. https://doi.org/10.1104/pp.15.01039

Tzin V, Hojo Y, Strickler SR, Bartsch LJ, Archer CM, Ahern KR, Zhou S, Christensen SA, Galis I, Mueller LA, *et al*. Rapid defense responses in maize leaves induced by *Spodoptera exigua* caterpillar feeding. *J Exp Bot*. 2017:68(16):4709–4723. https://doi.org/10.1093/jxb/erx274

Uraguchi S, Kato Y, Hanaoka H, Miwa K, Fujiwara T. Generation of boron-deficiency-tolerant tomato by overexpressing an *Arabidopsis thaliana* borate transporter AtBOR1. *Front Plant Sci*. 2014:5:125. https://doi.org/10.3389/fpls.2014.00125

Verwaaijen B, Alcock TD, Spitzer C, Liu Z, Fiebig A, Bienert MD, Bräutigam A, Bienert GP. The *Brassica napus* boron deficient inflorescence transcriptome resembles a wounding and infection response. *Physiol Plant*. 2023:175(6):1–18. https://doi.org/10.1111/ppl.14088

Warington K. The effect of boric acid and borax on the broad bean and certain other plants. *Ann Bot*. 1923:37(4):629–672. https://doi.org/10.1093/oxfordjournals.aob.a089871

Wilder SL, Scott S, Waller S, Powell A, Benoit M, Guthrie JM, Schueller MJ, Awale P, McSteen P, Matthes MS, *et al*. Carbon-11 radiotracing reveals physiological and metabolic responses of maize grown under different regimes of boron treatment. *Plants*. 2022:11(3):241. https://doi.org/10.3390/plants11030241

Wimmer MA, Goldbach HE. A miniaturized curcumin method for the determination of boron in solutions and biological samples. *J Plant Nutr Soil Sci*. 1999:162(1):15–18. https://doi.org/10.1002/(SICI)1522-2624(199901)162:1<15::AID-JPLN15>3.0.CO;2-P

Wouters FC, Gershenzon J, Vassão DG. Benzoxazinoids: reactivity and modes of action of a versatile class of plant chemical defenses. *J Braz Chem Soc*. 2016:27:1379–1397. https://doi.org/10.5935/0103-5053.20160177

Wu D, Tanaka R, Li X, Ramstein GP, Cu S, Hamilton JP, Robin Buell C, Stangoulis J, Rocheford T, Gore MA. High-resolution genome-wide association study pinpoints metal transporter and chelator genes involved in the genetic control of element levels in maize grain. *G3 (Bethesda, Md.)*. 2021:11(4):jkab059. https://doi.org/10.1093/g3journal/jkab059

Xu F, Wang Y, Meng J. Mapping boron efficiency gene(s) in *Brassica napus* using RFLP and AFLP markers. *Plant Breed*. 2001:120(4):319–324. https://doi.org/10.1046/j.1439-0523.2001.00583.x

Yan J, Shah T, Warburton ML, Buckler ES, Mcmullen MD, Crouch J. Genetic characterization and linkage disequilibrium estimation of a global maize collection using SNP markers. *PLoS One*. 2009:4(12):e8451. https://doi.org/10.1371/journal.pone.0008451

Zeng C, Han Y, Shi L, Peng L, Wang Y, Xu F, Meng J. Genetic analysis of the physiological responses to low boron stress in *Arabidopsis thaliana*. *Plant Cell Environ*. 2008:31(1):112–122. https://doi.org/10.1111/j.1365-3040.2007.01745.x

Zhang C, He M, Jiang Z, Liu T, Wang C, Wang S, Xu F. Arabidopsis transcription factor STOP1 directly activates expression of *NOD26-LIKE MAJOR INTRINSIC PROTEIN5;1*, and is involved in the regulation of tolerance to low-boron stress. *J Exp*. 2024:75:2574–2583. https://doi.org/10.1093/jxb/erae038

Zhang C, He M, Wang S, Chu L, Wang C, Yang N, Ding G, Cai H, Shi L, Xu F. Boron deficiency-induced root growth inhibition is mediated by brassinosteroid signalling regulation in Arabidopsis. *Plant J*. 2021:107(2):564–578. https://doi.org/10.1111/tpj.15311

Zhang H, Wang ML, Schaefer R, Dang P, Jiang T, Chen C. GWAS and coexpression network reveal ionomic variation in cultivated peanut. *J Agric Food Chem*. 2019:67(43):12026–12036. https://doi.org/10.1021/acs.jafc.9b04939

Zhao Z, Wu L, Nian F, Ding G, Shi T, Zhang D, Shi L, Xu F, Meng J. Dissecting quantitative trait loci for boron efficiency across multiple environments in *Brassica napus*. *PLoS One*. 2012:7(9):e45215. https://doi.org/10.1371/journal.pone.0045215